Design, synthesis, biological evaluation of 6-(2-amino-1*H*-benzo[*d*]imidazole- 6-yl)quinazolin-4(3*H*)-one derivatives as novel anticancer agents with Aurora kinase inhibition

Chengcheng Fan, Ting Zhong, Huarong Yang, Ying Yang, Daoping Wang, Xiaosheng Yang, Yongnan Xu, Yanhua Fan

PII: S0223-5234(20)30075-1

DOI: https://doi.org/10.1016/j.ejmech.2020.112108

Reference: EJMECH 112108

To appear in: *European Journal of Medicinal Chemistry*

Received Date: 29 October 2019

Revised Date: 11 January 2020

Accepted Date: 28 January 2020

Please cite this article as: C. Fan, T. Zhong, H. Yang, Y. Yang, D. Wang, X. Yang, Y. Xu, Y. Fan, Design, synthesis, biological evaluation of 6-(2-amino-1*H*-benzo[*d*]imidazole- 6-yl)quinazolin-4(3*H*)-one derivatives as novel anticancer agents with Aurora kinase inhibition, *European Journal of Medicinal Chemistry* (2020), doi: https://doi.org/10.1016/j.ejmech.2020.112108.

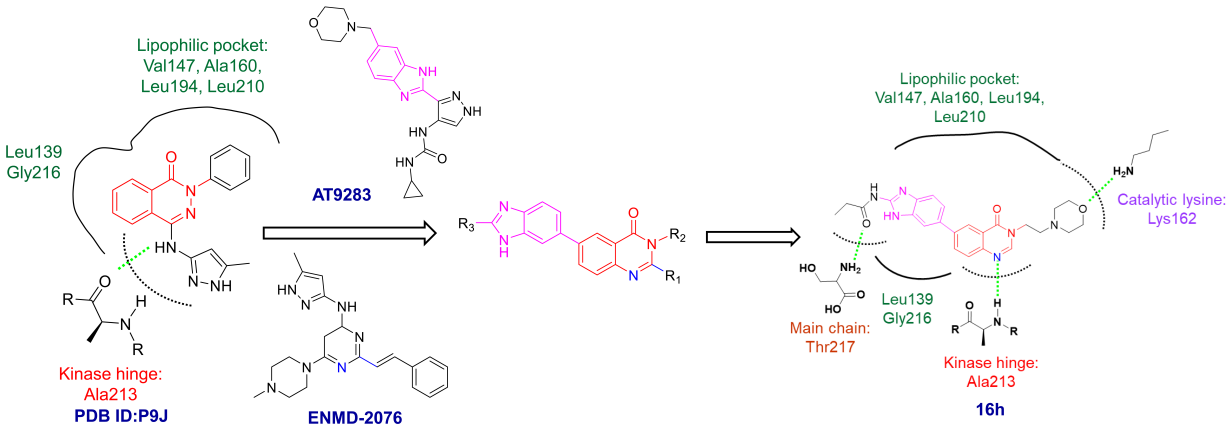

Aurora A: 21.94 nM
MDA-MB-231: 0.38 μM

Design, synthesis, biological evaluation of 6-(2-amino-1*H*-benzo[*d*]imidazol-6-yl)quinazolin-4(3*H*)-one derivatives as novel anticancer agents with Aurora kinase inhibition

Chengcheng Fan [b,c], Ting Zhong [a,b], Huarong Yang [b], Ying Yang [a,b], Daoping Wang [a,b], Xiaosheng Yang [a,b], Yongnan Xu [c,**], Yanhua Fan [a,b,*]

[a] State Key Laboratory for Functions and Applications of Medicinal Plants, Guizhou Medical University, Guiyang 550014, China.

[b] The Key Laboratory of Chemistry for Natural Products of Guizhou Province and Chinese Academy of Sciences, Guiyang 550014, China.

[c] Key Laboratory of Structure-Based Drug Design and Discovery, Ministry of Education, Shenyang Pharmaceutical University, Shenyang 110016, China.

[*] Corresponding author.

[**] Corresponding author.

Email addresses: fanyhkyem@163.com; ynxu@syphu.edu.cn.

Design, synthesis, biological evaluation of 6-(2-amino-1*H*-benzo[*d*]imidazol-6-yl)quinazolin-4(3*H*)-one derivatives as novel anticancer agents with Aurora kinase inhibition

Chengcheng Fan [b,c], Ting Zhong [a,b], Huarong Yang [b], Ying Yang [a,b], Daoping Wang [a,b], Xiaosheng Yang [a,b], Yongnan Xu [c,**], Yanhua Fan [a,b,*]

[a] State Key Laboratory for Functions and Applications of Medicinal Plants, Guizhou Medical University, Guiyang 550014, China.

[b] The Key Laboratory of Chemistry for Natural Products of Guizhou Province and Chinese Academy of Sciences, Guiyang 550014, China.

[c] Key Laboratory of Structure-Based Drug Design and Discovery, Ministry of Education, Shenyang Pharmaceutical University, Shenyang 110016, China.

Abstract

Aurora A kinase, a member of the Aurora kinase family, is frequently overexpressed in various human cancers. In addition, Overexpression of Aurora A kinase is associated with drug resistance and poor prognosis in many cancers including breast cancer. Therefore, Aurora A kinase has been considered as an attractive anticancer target for the treatment of human cancers. Herein, A series of 6-(2-amino-1*H*-benzo[*d*]imidazol-6-yl)quinazolin-4(3*H*)-one derivatives were

* Corresponding author.

** Corresponding author.

Email addresses: fanyhkyem@163.com; ynxu@syphu.edu.cn.

designed, synthesized, and evaluated as Aurora A kinase inhibitors. The cell-based cytotoxicity assays showed that compound **16h** was the most potent cytotoxic agent against all tested cancer cells and had a lower IC_{50} value than ENMD-2076 against MDA-MB-231 cells. Meanwhile, Aurora A kinase assay and Western blot analysis showed that **16h** inhibited Aurora A kinase with an IC_{50} value of 21.94 nM and suppressed the phosphorylation of Histone H3 on Ser10 and Aurora A kinase on Thr288, which were consistent with the activation of Aurora A kinase. Accordingly, **16h** caused aberrant mitotic phenotypes and obvious G2/M phase arrest in MDA-MB-231 cells and induced caspase-dependent apoptosis in MDA-MB-231 cells. These results demonstrated that **16h** is a potential candidate for the development of anticancer agents targeting Aurora A kinase.

Key word: Aurora A kinase; 6-(1*H*-benzo[*d*]imidazol-6-yl)quinazolin-4(3*H*)-one derivatives; cell cycle arrest; cell apoptosis

1. Introduction

The Aurora kinases (including Aurora A, B and C) are essential regulators of diverse cell cycle events in all eukaryotic organisms. Dysfunction of the Aurora kinases prevents cells from maintaining a stable chromosome content and contributes to tumorigenesis [1-2]. Aurora A kinase, which regulates maturation, mitotic spindle formation, and cytokinesis during mitosis, is frequently overexpressed in various human cancers [3-7], including colon, breast, pancreatic and ovarian tumors [8-12]. The inhibition of Aurora A kinase leads to mitotic catastrophe in cancer cells, which

eventually induces cell apoptosis [13-14]. Therefore, therapeutic inhibition of Aurora A kinase as an anticancer regime shows great promise because of the critical role of Aurora A kinase in division and proliferation of cancer cells [15]. In addition, overexpression of Aurora A kinase confers resistance to anticancer agents [16-18], including the epidermal growth factor receptor tyrosine kinase inhibitor (EGFR-TKI), cisplatin, Taxol and BRAF inhibitor, while the combination of Aurora A kinase inhibitors and these anticancer agents can delay the onset of drug resistances [19-22]. Hence, the development of Aurora A kinase inhibitors with minimal side effects and good pharmacological properties is an attractive platform for designing cancer therapeutics. In fact, numerous Aurora kinase inhibitors are currently under clinical trials including Aurora A specific inhibitors (Fig.1) [23-28]. However, the preclinical development of some Aurora A kinase inhibitors was limited by a narrow safety margin or other side effects [28]. Therefore, it's still urgent to develop new safe and effective Aurora A kinase inhibitors.

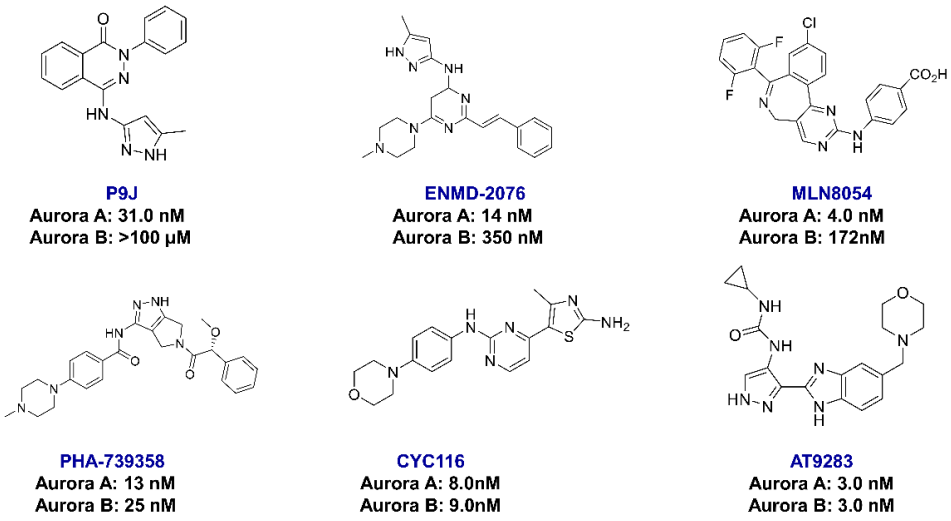

Fig. 1. Aurora A kinase inhibitors in clinical trials and P9J.

In this study, we intend to prepare a novel class of compounds that displays selective inhibitory for Aurora A kinase. Based on the binding mode of Aurora A and its specific inhibitors, the quinazolin-4(3*H*)-one and benzo[*d*]imidazole scaffolds were selected as a putative building block. As shown in Fig. 2, the aminopyrazole of **P9J** (a specific Aurora A inhibitor) formed key hydrogen bonding interactions with Ala213 in the hinge region of Aurora A, which are essential for maintaining the kinase activity and observed in most of the Aurora A kinase inhibitor complex structures [23-25]. As with the aminopyrazole of **P9J**, replacement the phthalazin-1-one moiety with quinazolin-4(3*H*)-one also formed hydrogen bonding interactions with Ala213. Quinazolin-4(3*H*)-one moiety is existing in nature products, such as febrigufine and isofebrifugine, and its derivatives were found to have distinctive biological functions [30]. Because quinazolin-4(3*H*)-one derivatives have various heterocyclic moieties and showed diverse bioactivities, it is possible to construct the modified and functional quinazolin-4(3*H*)-one-containing fragments as initial building block [30-33]. In addition, the benzo[*d*]imidazole, from which several Aurora kinase inhibitors had been built (e.g. AT-9238), has been proven to be a moiety with high efficiency against Aurora kinase [28, 34]. Based on these observations, a novel hybrid benzo[*d*]imidazole-quinazolinone was designed, synthesized and evaluated as Aurora A kinase inhibitors. In order to improve the kinase inhibitory activity, compounds were modified to further improve the physicochemical properties and binding affinity based on ligand-receptor interaction models of Aurora A kinase. Ultimately, a series of 6-(2-amino-1H-benzo[d]imidazol-6-yl)quinazolin-4(3H)-one derivatives were

obtained and identified. Furthermore, to examine the structure-activity relationships of these derivatives, structure modification was performed by introduction of various substituents at the C2-, N3- of quinazolin-4(3H)-one and the amino from 1H-benzo[d]imidazol-2-amine. Biological evaluation showed that compound **16h** displayed the best anticancer and Aurora A kinase inhibitor properties. Additionally, molecular docking studies, cell cycle distribution and cell apoptosis analysis were performed to explore the underlying anticancer mechanism of **16h**. These results demonstrated that **16h** is a promising candidate for the development of Aurora A kinase inhibitors.

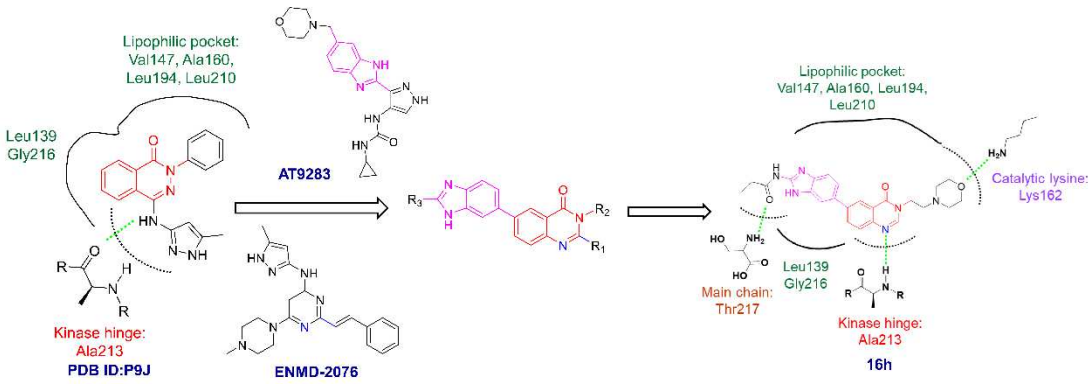

Fig. 2. Design of new scaffolds as Aurora A kinase inhibitors and the modification in the schematic active site of Aurora A kinase.

2. Results and discussion

2.1. Chemistry

The substituted quinazolin-4(3*H*)-one intermediates were synthesized from 2-amino-5-bromobenzoic acid. As shown in Scheme 1, three general methods A, B and C were used to synthesize the substituted quinazolin-4(3*H*)-one moiety [32-33].

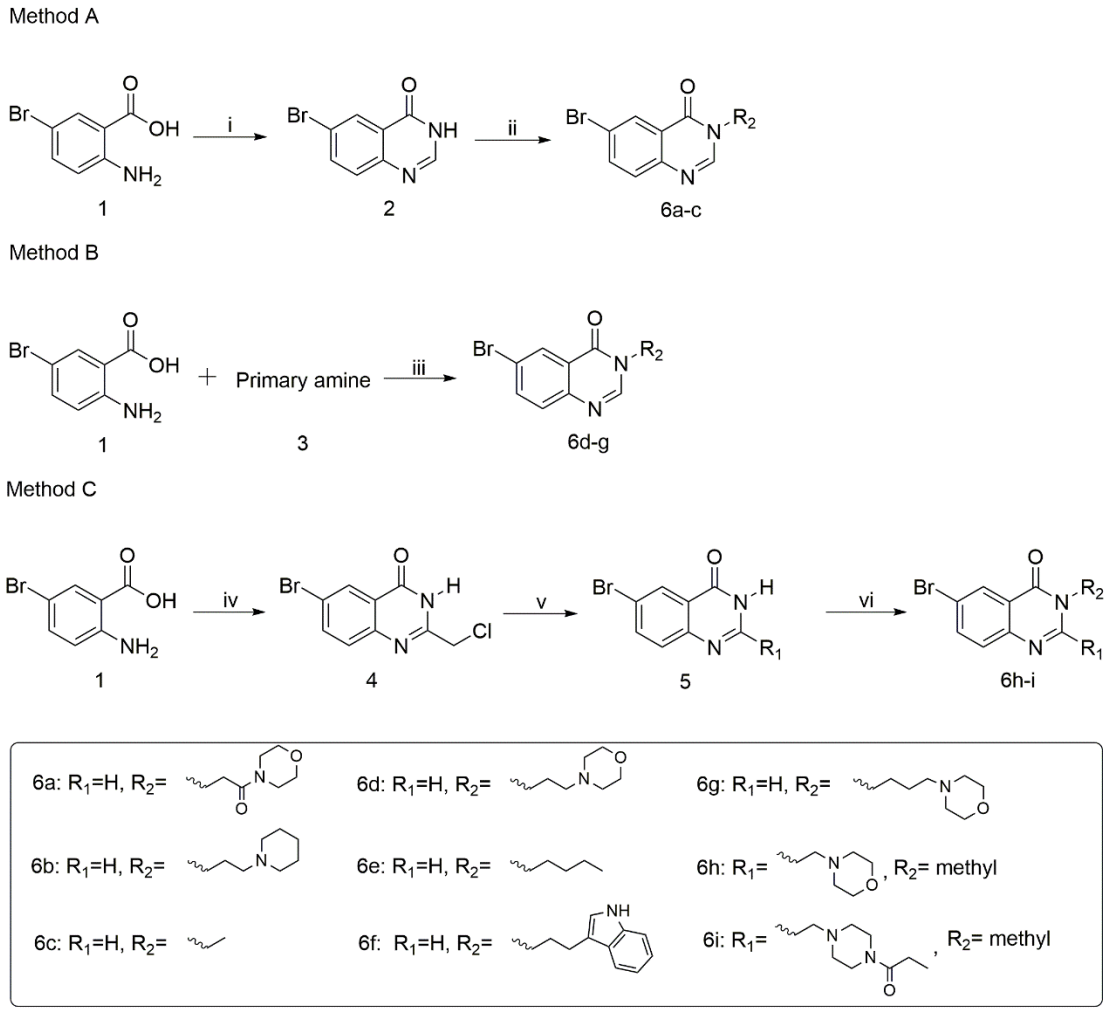

Scheme 1. (i) formamide, 130-135 ℃, 4 h; (ii) alkyl halides, NaH, DMF, ambient temperature, overnight; (iii) triethyl orthoformate, I_2, EtOH, reflux, 6 h; (iv) chloroacetonitrile, Na, MeOH, ambient temperature, 2 h; (v) amines, K_2CO_3, EtOH, reflux, overnight; (vi) alkyl halides, NaH, DMF, ambient temperature, overnight.

The alkylation of quinazolin-4(3*H*)-ones has been reported to afforded N^3-substituted products or a mixture of N^3- and O^4-substituted products. However, only N^3-substituted quinazolin-4(3*H*)-ones were obtained in this study according to the reported conditions [32]. After the quinazolin-4(3*H*)-ones moieties were constructed, the first step was to convert the C^6-bromo substituent of the quinazolin-4(3*H*)-ones into the 4,4,5,5-tertramethyl-1,3,2-dioxaborolane, and these intermediates were then used to prepare the final products via a Suzuki Coupling

Reaction with 1*H*-benzo[d]imidazole moiety. As shown in Scheme 2, even though the preparation of quinazolin-4(3*H*)-one borate esters **7e** afforded high yields, the homo-coupling byproduct (product **9)** rather than the desired cross-coupling product **8** was finally obtained. Then, we tried to convert compound **10c** to corresponding borate esters **10** via Miyaura reaction. Unfortunately, **10** was not gained as we had expected.

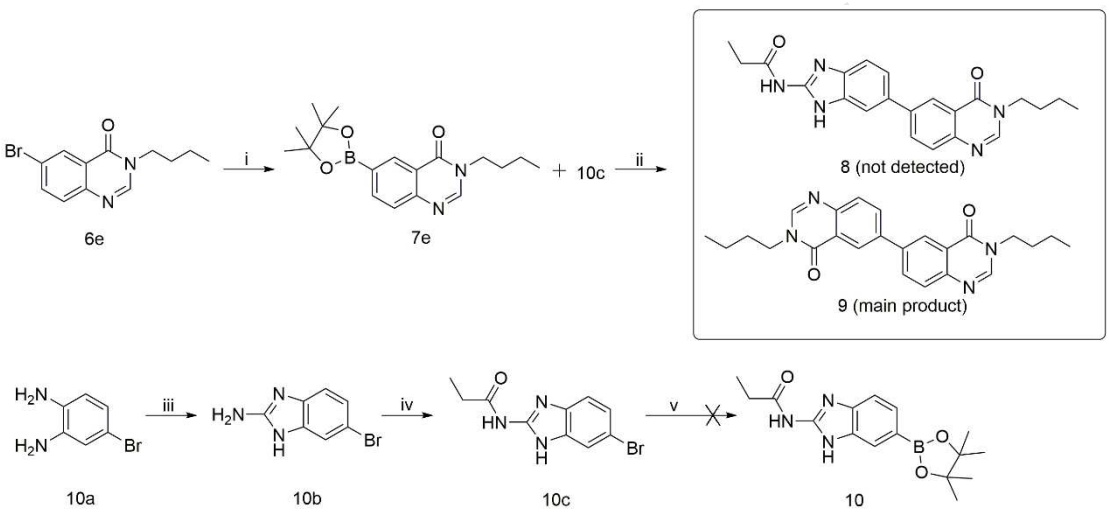

Scheme 2.: (i) bis(pinacolato)diborane, Pd(dppf)Cl_2, AcOK, Dioxane, 100 ºC, 2 h; (ii) Pd(dppf)Cl_2, K_2CO_3 , Dioxane/H_2O, 100 ℃, 20 h; (iii) CNBr, MeOH/H_2O, 60 ℃, 5 h; (iv) Propionyl chloride, Et_3N, THF, 0 ℃ to ambient temperature, 5 h; (v) bis(pinacolato)diborane, Pd(dppf)Cl_2, AcOK, dioxane, 100 ºC, 24 h.

To obtain the final products bearing the 6-(2-amino-1*H*-benzo[*d*]imidazol-6-yl)quinazolin-4(3*H*)-one as skeleton and verify our conjecture that the quinazolin-4(3*H*)-one fragments are much more reactive than the *N*-(6-bromo-1*H*-benzo[*d*]imidazol-2-yl)amide fragments, an alternative synthetic strategy was applied, as shown in the Scheme 3. Critical intermediate **13** were prepared via a Suzuki-Miyaura Cross-Coupling reaction. 6-bromoquinazolin-4(3*H*)-ones was treated

with 2-nitro-4-(4,4,5,5-tetramethyl-1,3,2-dioxaborolan-2-yl)aniline, which was obtained from 4-bromo-2-nitroaniline, to afford intermediate **13**, and Pd(dppf)Cl_2 was chosen as a highly efficient catalyst. Interestingly, the yields of the borate esters from the Miyaura reactions are more than 90%, and the cross-coupling reactions afford the crucial intermediates **13** in good yields (above 80%). Pd/C was utilized as catalyst for the reduction of the nitro group and yielded corresponding *o*-phenylenediamine compounds **14** with nearly full conversion [35-37]. Subsequently, compounds **15** were obtained by treating compounds **14** with BrCN using a direct one-step synthetic method to produce the corresponding 6-(2-amino-1*H*-benzo[*d*]imidazol-6-yl)-quinazolin-4(3*H*)-ones [37-38]. Finally, the treatment of compounds **15** with different acyl chlorides resulted in target compounds **16**. Various substituents were introduced at the C^2- and N^3-positions of the quinazolin-4(3*H*)-one scaffold. Various amide, urea and carbamate derivatives were also synthesized to further explore the structure-activity relationship. All compounds are shown in Table 1.

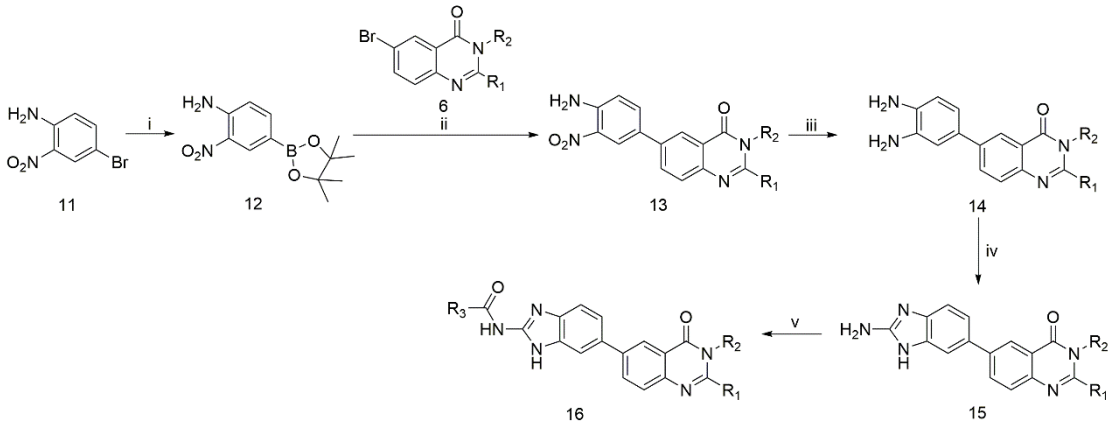

Scheme 3. (i) bis(pinacolato)diborane, Pd(dppf)Cl_2, AcOK, dioxane, 100 ºC, 2 h; (ii) substituted quinazolin-4(3*H*)-one, Pd(dppf)Cl_2, K_2CO_3 ,dioxane/H_2O, 100 ℃, 5 h; (iii) $NH_2NH_2 \cdot H_2O$, Pd/C, MeOH, 80 ℃, 2 h; (iv) CNBr, MeOH/H_2O, 60 ℃, 5 h; (v) Acyl chloride, Et_3N, THF, 0 ℃ to ambient temperature, overnight.

Table 1. Cytotoxic activity (IC_{50}, μM) [a] against cancer cell lines.

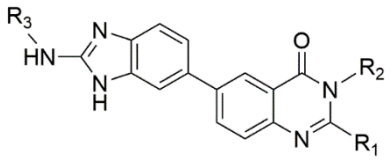

Comp.	R_1	R_2	R_3	MDA-MB-231	PC3	SH-SY5Y
16a	H	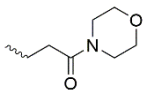		>20	>20	>20
16b	H	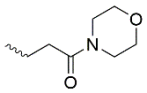		>20	>20	>20
16c	H			13.5±0.18	>20	18.13±0.28
16d	H			>20	>20	>20
16e	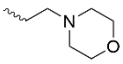			0.94±0.14	1.65±0.23	1.08±0.19
16f	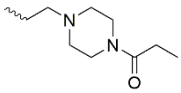			>20	>20	5.49±0.42
16g	H	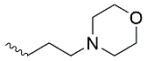		>20	>20	>20
16h	H	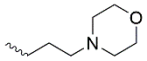		**0.38±0.08**	**1.09±0.24**	**0.77±0.12**
16i	H	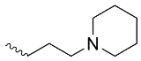		1.23±0.09	6.57±1.02	4.02±0.98
16j	H	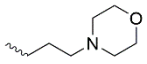	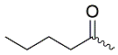	3.85±0.28	6.54±1.08	4.19±0.79
16k	H	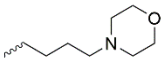		1.22±0.23	3.21±0.25	1.68±0.16
16l	H	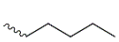		>20	>20	>20
16m	H	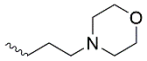		>20	>20	>20
16n	H	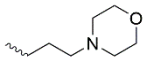		4.85±0.69	6.45±0.21	3.92±0.24
16o	H	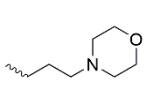		1.76±0.17	8.13±0.92	2.52±0.31

16p	H	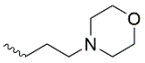		1.61±0.21	11.2±1.08	7.33±0.67
16q	H	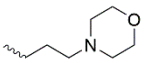		10.2±1.56	16.5±2.89	14.2±2.11
16r	H	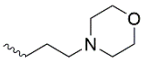		>20	>20	>20
16s	H	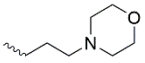	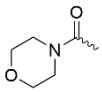	>20	>20	>20
16t	H	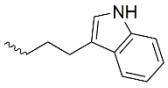		0.55±0.10	1.67±0.12	1.23±0.19
ENMD-2076	-	–	-	0.48±0.09	0.67±0.11	NT

[a] IC_{50} values are the mean of triplicate measurements. NT: not tested.

2.2. Biological evaluation

2.2.1. Cytotoxicity

To test the cytotoxicity of the synthesized compounds, an MTT assay was employed to measure their anticancer activities against various human cancer cell lines, including breast cancer MDA-MB-231, prostate cancer PC3, and neuroblastoma SH-SY5Y cells. As shown in Table 1, most of the synthesized compounds displayed potent antiproliferative activity against the three cancer cell lines. Among them, **16h** showed the strongest inhibitory potency against MDA-MB-231 cells with an IC_{50} value of 0.38 μM. In addition, the proliferation of cells treated with **16h** for 48 h was inhibited in a dose-dependent manner, and some typical morphological features of apoptotic cells, such as shrinkage and blebbing, were observed in the cells treated with **16h** above 1.0 μM (Fig. 3A). Colony formation was also significantly inhibited by **16h** (Fig. 3B), which is consistent with the growth-inhibitory activity results from

the MTT assay. According to the results of the MTT assay, compared with **16h**, compounds **16e** and **16f**, containing a methyl group at N^3 and a substituent at C^2, showed weaker activities against all the tested cancer cell lines. This indicated that the replacement of the morpholinoethyl moiety at N^3 with a methyl group might decrease the anticancer activity. In addition, the replacement of morpholino ethyl with (1*H*-indol-2-yl) ethyl (**16t**) can decrease both the anticancer activity and the water solubility. The introduction of an electron-withdrawing carbonyl in the morpholinoethyl side chain significantly reduced the activity (**16a**, **16b**). Extended the alkyl side chain of the propenamide at the 2-position of the benzimidazole (**16j**) or increased the steric hindrance due to the introduction of a macrocyclic substituent (**16p**-**16s**) may diminished the anticancer activity. Although replacement of the propenamide with groups containing carbamate or urea fragments (**16m**-**16o**) further improved the water solubility, the activities were decreased. The replacement of the propenamide with ethyl sulfonamide, an electron withdrawing group, at the 2-substituent of benzimidazole (**16a** and **16g**) also significantly reduced the anticancer activity.

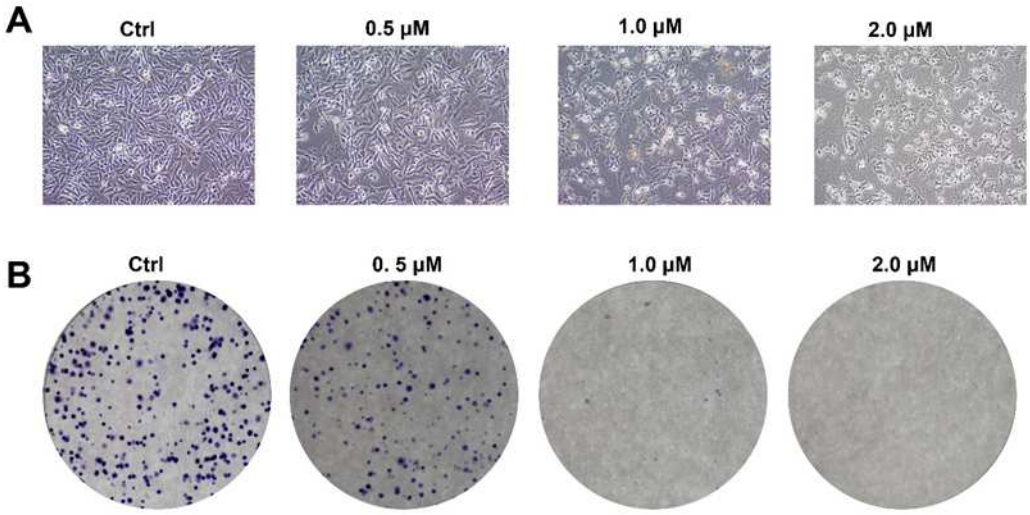

Fig. 3. The effects of **16h** on cell proliferation. (A) The cell proliferation and morphologic changes after **16h** treatment for 48 h. (B) **16h** inhibited the capacity of colony formation of MDA-MB-231 cells. 500 cells were plated in 6 wells plates and incubated for 12 h before treatment with DMSO or **16h** at indicated concentration for 72 h. Then cells were washed once with PBS and continue to culture with full-growth medium for 10 days, change the culture medium to fresh ones every three days. Cells were stained with 0.1% crystal violet after fixing with 100% methanol.

*2.2.2. **16h** inhibited Aurora kinase activity*

To elucidate whether the antiproliferative activity of the synthesized compounds is associated with Aurora kinase, an Aurora kinase assay was conducted to test the kinase inhibitory activity of **16h** against Auroras A and B. As shown in Table 2, **16h** exhibited excellent inhibitory activities against Aurora A kinase with an IC_{50} value of 21.94 nM, but much lower activity against Aurora B kinase with an IC_{50} value of 273.18 nM. In addition, Western blot analysis was used to further examine the effects of **16h** on the expression of phospho-Aurora A at Thr288 which is a critical residue for activating phosphorylation events in its catalytic domain. The phospho-Histone

H3 at Ser10 was also detected, a downstream target of Aurora kinase. As depicted in Fig. 4, upon treatment with **16h** for 24 h, a dose-dependent and significant reduction in the phosphorylation of Aurora A and Histone H3 was observed in MDA-MB-231 cells, which is consistent with the effects of other inhibitors of Aurora kinase [39-40].

Table 2. Aurora kinase inhibition by 16t and 16h.

Compound	Aurora A kinase inhibition (IC_{50}) [a]	Aurora B kinase inhibition (IC_{50}) [a]
16t	27.12 nM	329.81 nM
16h	21.94 nM	273.18 nM
ENMD-2076	15.28 nM	293.72 nM
Staurosporine	18.09 nM	26.13 nM

[a] IC_{50} values are the mean of triplicate measurements.

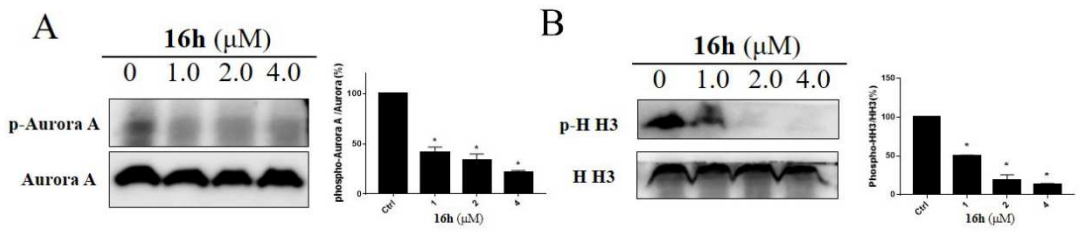

Fig. 4. Aurora A kinase inhibition by **16h**. (A) **16h** decreased the phospho-Aurora A kinase at Thr288. (B) **16h** decreased the phospho-Histone H3 at Ser10. Cells were exposed to DMSO or **16h** at indicated concentrations for 24 h and then were collected for Western blot analysis. The changes in corresponding protein expression levels were quantified using Image J. Each bar represents the mean ± SEM (n = 3); *P < 0.05 or **P < 0.01 was considered statistically significant compared with the corresponding control values.

To predict the binding model of the active compounds with Aurora A kinase, molecular docking simulation was performed using Autodock 4.2. According to the results of the molecular docking study, **16h** showed the best docking score and binding affinities with Aurora A kinase. The docking information of **16h** with Aurora A kinase was analyzed. Analysis of the protein-ligand interactions in the co-crystal

with the ligand of Aurora A showed that the common interaction patterns include the following: the nitrogen atom of the morpholine ring, the benzimidazoles and the amide side chains of **16h** formed conserved hydrogen bonds with amino acid residues Ala213 in the kinase hinge region, the main chain NH of Thr217 and the catalytic lysine of Lys162. Compared with **16t** and P9J (the co-crystal ligand of Aurora A), **16h** formed two extra hydrogen bones with Thr217 and Lys162 in the active site to further stabilize the interactions with Aurora A. In addition, the quinazolinone fragment formed hydrophobic interactions including π-π stacked and π-alkyl interactions with residues including Leu139, Ala160, Leu194, Leu210, Ala213 and leu263 of Aurora A (Fig. 5). In summary, the molecular docking study also predicted the potential inhibitory activity of **16h** against Aurora A.

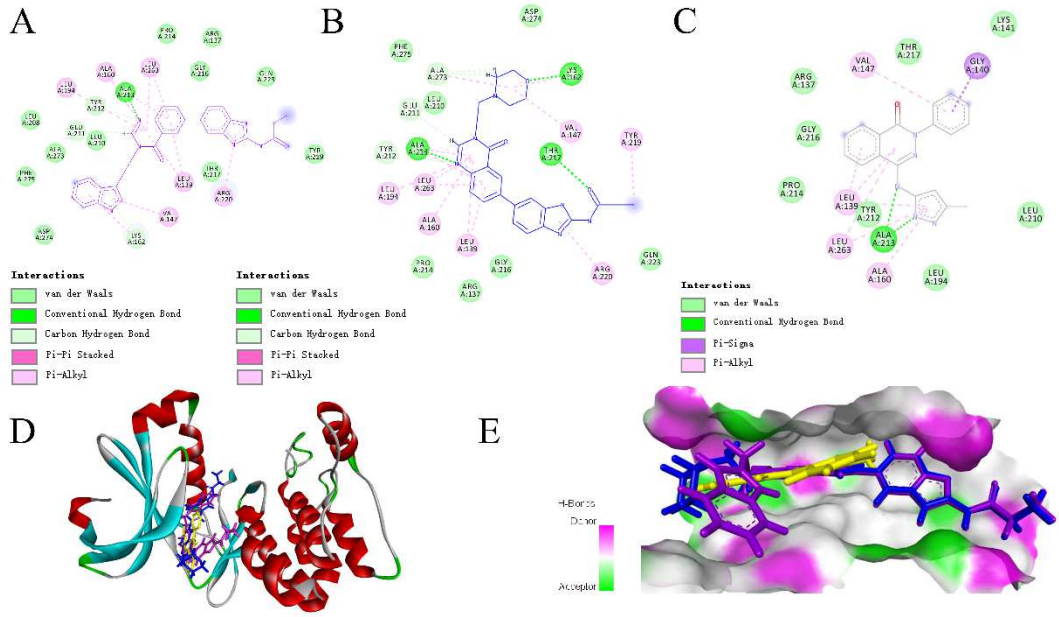

Fig.5. Proposed binding mode of compound **16h** and in the active site of Aurora A kinase (PDB ID code:3P9J). (A) The 2D binding model of **16t** and Aurora A kinase. (B) The 2D binding model of **16h** and Aurora A kinase. (C) The 2D binding model of the co-crystal ligand and Aurora A kinase. (D) The 3D binding conformation of **16h** (blue), **16t** (purple) and the co-crystal ligand (yellow) in the active site of Aurora A kinase. (E) Structural overlay

of the complexes: **16h** (blue), **16t** (purple) and co-crystal ligand of Aurora A kinase (yellow) in the ligand-binding pocket. The figure was generated using Accelrys Discovery Studio Visualizer 4.5.

*2.2.3 **16h** induced G2/M cell cycle arrest*

Aurora kinases are critical regulators throughout the cell cycle and Aurora A is usually responsible for mediation the G2/M transition [40-41]. To further confirm the effects of **16h** on Aurora A kinase, the cell cycle distribution of MDA-MB-231 cells was examined after treatment with **16h**, the most highly active compounds, for 24 h. As shown in Fig. 6, significant G2/M transition arrest was observed in MDA-MB-231 cells treated with **16h**. The Fraction of cells in the G2/M phase was dose-dependently increased by the treatment with **16h**, and the population of cells in the G2/M phase was markedly increased to 76.19% in 5μM **16h**-treated cells compared to 16.62% in untreated cells.

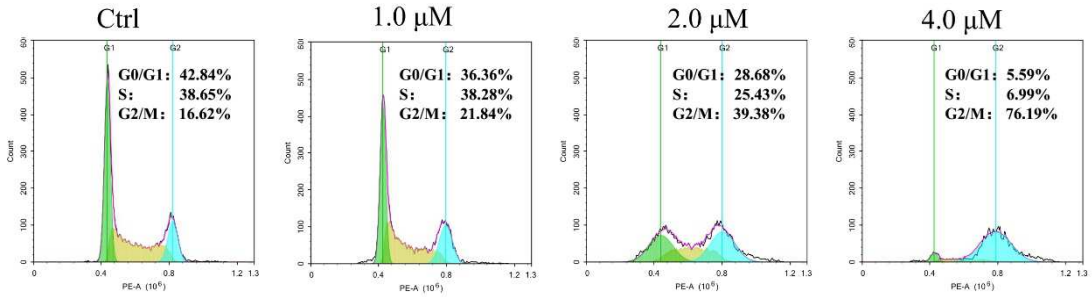

Fig 6. 16h induced cell cycle arrest at G2/M phase. **16h** altered cell cycle distribution in MDA-MB-231 cells. Cells were exposed to DMSO or **16h** at indicated concentrations for 24 h and then were collected for DNA content analysis by flow cytometric analysis as experiment.

*2.2.4 **16h** induced apoptosis of MDA-MB-231 cells*

To determine whether the antiproliferative activity of **16h** was accompanied by enhanced cancer cell apoptosis, cell apoptosis was detected by a flow cytometry assay

after staining with an Annexin V-FITC apoptosis detection kit. Cells treated with **16h** at 2.0 μM and 4.0 μM displayed significant increases in the percentage of Annexin-V-positive cells, from 6.42% in the vehicle control to 19.86% for 2.0 μM and 30.74% for 4.0 μM **16h**-treated cells. The changes in apoptotic proteins were further evaluated, including cleaved caspase 3/9 and cleaved-PARP. As expected, **16h** significantly increased the levels of all three cleaved proteins (Fig. 7). Hence, these observations demonstrated that compound **16h** induced obvious apoptosis in MDA-MB-231 cells in a concentration-dependent manner.

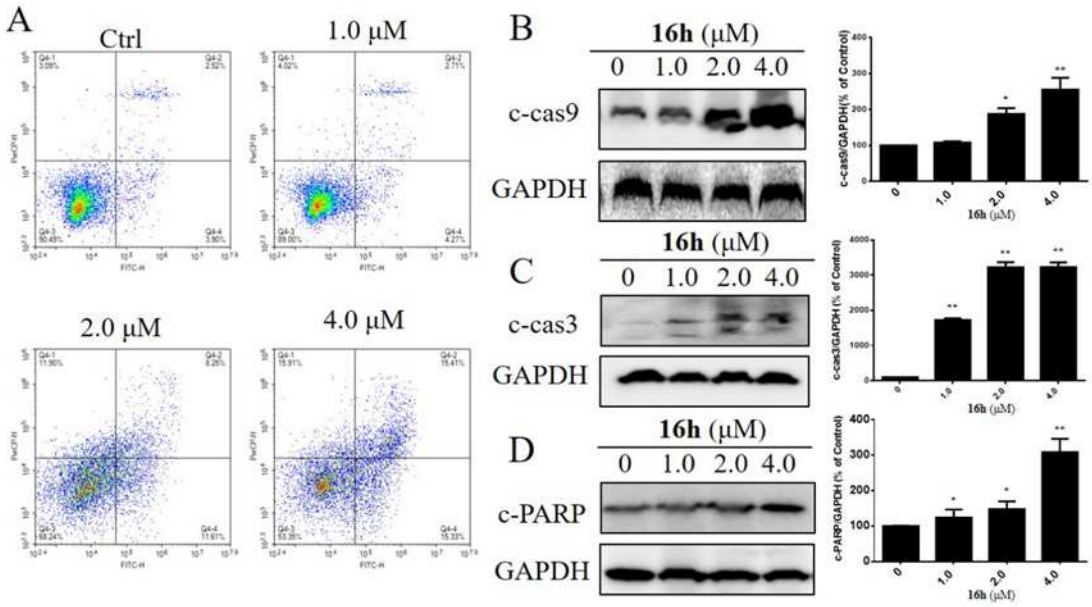

Fig.7. 16h induced apoptosis in MDA-MB-231 cells. (A) Cell apoptosis was analyzed by flow cytometric analysis after Annexin V-FITC/PI staining. Cells were collected and centrifuged at 1500 rpm for 10min after compound **16h** treatment at the indicated concentrations for 48 h. (B-D**)** The effect of **16h** on the induction of apoptosis was also analyzed by Western blot in MDA-MB-231 cells. The changes in corresponding protein expression levels were quantified using Image J. Each bar represents the mean ± SEM (n = 3). *P < 0.05 or **P < 0.01 was considered statistically significant compared with the corresponding control values.

3. Conclusions

In the present study, a series of 6-(1*H*-benzo[*d*]imidazol-6-yl)-3-quinazolin-4(3*H*)-one derivatives were synthesized and biologically evaluated. Among them, compound **16h** exhibited the strongest antiproliferative activity against the tested cancer cells lines. Further mechanistic studies showed that **16h** exhibited antiproliferative activity and induced G2/M phase cell cycle arrest and cell apoptosis via Aurora kinase inhibition and the mitochondrial apoptotic pathway.

4. Experimental

4.1. Chemistry

All reagents and solvents were commercially available and were used without further purification. ^{1}H NMR and ^{13}C NMR spectra were recorded on a Bruker AVANCE NEO 600 MHz NMR spectrometer and the NMR spectra was generated using Mestrenova 12.0 as processing software. Spectra were recorded at 25□ using dimethyl sulfoxide-d_6 and methanol-d_4 as solvents with tetramethylsilane (TMS) as an internal standard. All chemical shifts are reported in ppm (δ), and coupling constants (J) are in hertz (Hz). All the melting points were determined on a Beijing micro melting-point apparatus, and the values are uncorrected. High-resolution exact mass measurements were performed using electrospray ionization (positive mode) on a quadrupole time-of-flight (QTOF) mass spectrometer (microTOF-Q, Bruker Inc.). The structures of compounds **16a** to **16t** were confirmed based on ^{1}H and ^{13}C NMR spectroscopy, HR-MS and element analysis. The HMBC and HMQC data of compound **16h** were used to characterize the series of compounds, although several carbon signals were undetectable in the ^{13}C NMR spectra of some derivatives.

4.1.1. Preparation of 6- bromo-N^3-substituted quinazolin-4(3H)-ones, Method A.

A mixture of 2-amino-5-bromobenzoic acid (2.16 g, 10 mmol) and formamide (1.80 g, 40 mmol) was heated at 130-135 °C. After the mixture had been stirred for 4 h, water (30 mL) was added. The reaction mixture was cooled to 60 °C, and additional water 20 mL was added to the mixture. After stirring the mixture for another 30 min, the precipitated product was separated by vacuum filtration. The crude products were recrystallized from ethanol to give 6-bromoquinazolin-4(3*H*)-one **2** in yields of 80-95%. To a solution of compound **2** (1.125 g, 5 mmol) in anhydrous DMF 15 mL under argon was added NaH (60% dispersion in mineral oil, 0.24 g, 6 mmol) in one portion. The reaction mixture was stirred at room temperature for 3 min, and then 2-chloro-1-morpholinoethan-1-one (1.145 g, 7 mmol) was added dropwise. The reaction mixture was stirred at room temperature overnight and then partitioned between EtOAc (100 mL) and brine (100 mL). The organic layer was washed with more brine (100 mL). The combined aqueous washings were extracted with EtOAc (3×75 mL). The combined AcOEt extracts were washed with brine (2×100 mL), dried (Na_2SO_4), and concentrated in vacuo. Purification by column chromatography eluting with EtOAc / PE, afforded 6-bromo-3-(2-morpholino-2-oxoethyl)quinazolin-4(3*H*)-one **6a** as a white solid (1.21 g, 3.44 mmol, 68.8 % yield). ESI-MS: *m/z* 352.0, 354.0 $[M+H]^+$.

Compound ***6b*** **-** ***6c*** was synthesized according to the procedure described in ***6a***.

*4.1.2. 6-bromo-3-(2-(piperidin-1-yl)ethyl)quinazolin-4(3H)-one (**6b**).*

Yellow solid, 62.5% yield. ESI-MS: *m/z* 336.0, 338.0 $[M+H]^+$.

*4.1.3. 6-bromo-3-methylquinazolin-4(3H)-one (**6c**).*

White solid, 73.3% yield. ESI-MS: *m/z* 260.9, 262.9 $[M+Na]^+$.

4.1.4. Preparation of 6-bromo-N^3-substituted quinazolin-4(3H)-ones, Method B.

The mixture of 2-amino-5-bromobenzoic acid (2.16 g, 10 mmol), triethyl orthoformate (1.93 g, 13 mmol), 2-morpholinoethan-1-amine (1.69 g, 13 mmol), iodine (0.025 g, 0.1 mmol) and anhydrous ethanol 30 (mL) was refluxed under argon atmosphere for 4 - 6 h, then concentrated under vacuum to give a residue which was dissolved in ethyl acetate (100 mL). The ethyl acetate solution was washed with 1 N aqueous sodium hydroxide (50 mL×3) and brine (50 mL×3), dried over anhydrous sodium sulfate and concentrated to give 6-bromo-3-(2-morpholinoethyl)quinazolin-4(3*H*)-one **6d** as yellow solid (2.755 g, 8.15 mmol, 81.5% yield). ESI-MS: *m/z* 338.0, 340.0 $[M+H]^+$.

Compounds **6e - 6g** were synthesized according to the procedure described in **6d**.

*4.1.5. 6-bromo-3-butylquinazolin-4(3H)-one (**6e**).*

White solid, 81.1% yield. ESI-MS *m/z*: 281.0, 283.0 $[M+H]^+$.

*4.1.6. 3-(2-(1H-indol-3-yl) ethyl)-6-bromoquinazolin-4(3H)-one (**6f**).*

White solid, 65.0% yield. ESI-MS: *m/z* 368.0, 370.0 $[M+H]^+$.

*4.1.7. 6-bromo-3-(3-morpholinopropyl)quinazolin-4(3H)-one (**6g**).*

White solid, 71.3% yield. ESI-MS: *m/z* 352.2, 354.2 $[M+H]^+$.

4.1.8. Preparation of 6- bromo-C^2, N^3-substituted quinazolin-4(3H)-ones, Method C.

To a flask containing sodium (69 mg, 3 mmol) was added anhydrous MeOH (10 mL), then chloroacetonitrile (3.40 g, 45 mmol) with a syringe via a rubber septum,

and the solution was stirred at ambient temperature for about 40 min under argon. A solution of 2-amino-5-bromobenzoic acid (3.24 g, 15 mmol) in anhydrous MeOH (30 mL) was then added. The reaction mixture was stirred at this temperature for about 2 h under argon. The precipitate was collected by filtration, washed by MeOH (15 mL) and H_2O (10 mL), and MeOH (15mL), then the white filter residue was dried under vacuum at room temperature to obtain the 6-bromo-2-(chloromethyl)quinazolin-4(3*H*)-one **4** as pure white solid. A solution of **4** (1.37 g, 5 mmol) in EtOH (25 mL) was added morpholine (0.52 g, 6 mmol) slowly in a three-necked flask and stirred for 30 minutes at room temperature, then K_2CO_3 (1.38 g, 10 mmol) was added to the bottle in batches. After that, the mixture were heated to reflux and stirred overnight. After the reaction completed (monitored by TLC), The crude reaction mixture was cooled and EtOH were removed under reduced pressure and add water (100 ml), extracted with ethyl acetate (3×100 ml), the organic layer was washed with water (3×100 ml), dried with Na_2SO_4 and evaporated, the residue was purified through a column chromatography on silica with EtOAc/PE to afford white solid, 6-bromo-2-(morpholinomethyl)quinazolin-4(3*H*)-one. With this intermediate in hand, 6-bromo-3-methyl-2-(morpholinomethyl)quinazolin-4(3*H*)-one **6h** was obtained from compound **5** which was treated with CH_3I under the condition described in Method B, as white solid, 63% yield of three steps. ^{1}H NMR (600 MHz, DMSO-d_6) δ 8.23 (d, J = 2.3 Hz, 1H), 7.97 (dd, J = 8.7, 2.3 Hz, 1H), 7.64 (d, J = 8.7 Hz, 1H), 5.75 (s, 2H), 3.65 (t, J = 4.6 Hz, 4H), 3.51 (s, 3H), 2.56-2.49 (m, 4H). ESI-MS: *m/z* 360.0, 362.0 $[M+Na]^+$

Compound **6i** was synthesized according to the procedure described in **6h**.

*4.1.9. 6-bromo-3-methyl-2-((4-propionylpiperazin-1-yl)methyl)quinazolin-4(3H)-one (**6i**)*

White solid, 61.2% yield. ESI-MS: *m/z* 415.0, 417.0 $[M+Na]^+$.

*4.1.10. 2-nitro-4-(4,4,5,5-tetramethyl-1,3,2-dioxaborolan-2-yl)aniline (**12**)*

A solution of the 4-bromo-2-nitroaniline (1.63 g, 7.5 mmol), KOAc (2.21 g, 22.5 mmol), bis(pinacolato)diborane (3.81 g, 15 mmol) and $Pd(dppf)_2Cl_2$ (0.28 g, 0.38 mmol) in anhydrous 1,4-dioxane (30 ml) under argon was stirred at 100 □ for 2 h. 1,4-dioxane was removed under reduced pressure and add water (100 ml), extracted with ethyl acetate (3×100 ml), the organic layer was washed with water (2×100 ml), dried with Na_2SO_4 and evaporated to give as a yellow solid and used for next step without another purification (>90% yield).

*4.1.11. General procedure of preparation of compounds 6-(4-amino-3-nitrophenyl)-quinazolin-4(3H)-ones (**13**).*

A solution of 2-nitro-4-(4,4,5,5-tetramethyl-1,3,2-dioxaborolan-2-yl)aniline **12** (1.32 g, 5 mmol), 6-bromoquinazolin-4(3*H*)-ones **6** (5 mmol) , and K_2CO_3 (2.07 g, 15 mmol) , 1,4-dioxane/water 25 mL [V(dioxane):V(water) = 4:1] mixture as solvent was heated to 100 □ and stirred for 15 min. $Pd(dppf)Cl_2$ (0.18 g, 0.25 mmol) was added, and the mixture was continued stirred at this temperature under argon for another 4-6 h. 1, 4-dioxane and water was removed under reduced pressure and the residue was purified through a column chromatography on silica with dichloromethane/methanol to afford bright yellow solid.

*4.1.12. 6-(4-amino-3-nitrophenyl)-3-(2-morpholino-2-oxoethyl)quinazolin-4(3H)-one (**13a**).*

Yellow solid, 86.0% yield. ^{1}H NMR (600 MHz, DMSO-d_6) δ 8.31 (d, J = 2.3 Hz, 1H), 8.26 (s, 1H), 8.15 (dd, J = 8.5, 2.3 Hz, 1H), 7.82 (d, J = 1.8 Hz, 1H), 7.79 (d, J = 8.5 Hz, 1H), 7.59 (dd, J = 8.2, 1.8 Hz, 1H), 7.37 (d, J = 8.2 Hz, 1H), 7.09 (bs, 2H), 4.98 (s, 2H), 3.69, 3.48 (t, J = 4.9, 4H), 3.63-3.57 (m, 4H). ESI-MS: *m/z* 432.1 $[M+Na]^+$.

*4.1.13. 6-(4-amino-3-nitrophenyl)-3-(2-(piperidin-1-yl)ethyl)quinazolin-4(3H)-one (**13b**).*

Yellow solid, 81.3% yield. ^{1}H NMR (600 MHz, DMSO-d_6) δ 8.31 (s, 1H), 8.18 (d, J = 2.3 Hz, 1H), 8.00 (dd, J = 8.5, 2.3 Hz, 1H), 7.65-7.63 (m, 1H), 7.61 (d, J = 8.4 Hz, 1H), 7.39 (d, J = 8.3 Hz, 1H), 7.33 (dd, J = 8.3, 1.8 Hz, 1H), 7.09 (s, 2H), 4.30 (t, J = 6.7 Hz, 2H), 3.20 (s, 4H), 2.80 (s, 2H), 2.32 (t, J = 7.6 Hz, 2H), 1.64 (d, J = 6.8 Hz, 4H). ESI-MS: *m/z* 416.2 $[M+Na]^+$.

*4.1.14. 6-(4-amino-3-nitrophenyl)-3-methylquinazolin-4(3H)-one (**13c**).*

Yellow solid, 82.1% yield. ^{1}H NMR (600 MHz, DMSO-d_6) 8.37 (s, 1H), 8.35 (d, J = 2.3 Hz, 1H), 8.12 (dd, J = 8.7, 2.3 Hz, 1H), 7.81 (bs, 1H), 7.74 (d, J = 8.5 Hz, 1H), 7.55 (d, J = 8.3 Hz, 1H), 7.50-7.48 (dd, J = 8.3, 1.8 Hz, 1H), 7.10 (s, 2H), 3.53 (s, 3H), ESI-MS: *m/z* 297.0 $[M+H]^+$.

*4.1.15. 6-(4-amino-3-nitrophenyl)-3-(2-morpholinoethyl)quinazolin-4(3H)-one (**13d**).*

Yellow solid, 81.1% yield. ^{1}H NMR (600 MHz, DMSO-d_6) δ 8.34 (s, 1H), 8.33 (d, J = 2.2 Hz, 1H), 8.13 (dd, J = 8.5, 2.2 Hz, 1H), 7.81 (d, J = 1.5 Hz, 1H), 7.76 (d, J

= 8.5 Hz, 1H), 7.59 (dd, *J* = 8.2, 1.7 Hz, 1H), 7.36 (d, *J* = 8.2 Hz, 1H), 7.08 (s, 2H), 4.12 (t, *J* = 6.1 Hz, 2H), 3.53 (t, *J* = 4.6 Hz, 4H), 2.63 (t, *J* = 6.1 Hz, 2H), 2.45 (bs, 4H). ESI-MS: *m/z* 418.2 $[M+Na]^+$.

*4.1.16. 6-(4-amino-3-nitrophenyl)-3-butylquinazolin-4(3H)-one (**13e**)*

Yellow solid, 82.3% yield. ESI-MS: *m/z* 361.1 $[M+Na]^+$.

*4.1.17. 3-(2-(1H-indol-3-yl)ethyl)-6-(4-amino-3-nitrophenyl)quinazolin-4(3H)-one (**13f**).*

Yellow solid, 89.4% yield. ESI-MS: *m/z* 448.1 $[M+Na]^+$.

*4.1.18. 6-(4-amino-3-nitrophenyl)-3-(3-morpholinopropyl)quinazolin-4(3H)-one (**13g**).*

Yellow solid, 80.3% yield. ESI-MS: *m/z* 432.2 $[M+Na]^+$.

*4.1.19. 6-(4-amino-3-nitrophenyl)-3-methyl-2-(morpholinomethyl)quinazolin-4(3H)-one (**13h**).*

Yellow solid, 82.8% yield. ESI-MS: *m/z* 418.1 $[M+Na]^+$.

*4.1.20. 6-(4-amino-3-nitrophenyl)-3-methyl-2-((4-propionylpiperazin-1-yl)methyl) quinazolin-4(3H)-one (**13i**).*

Yellow solid, 88.9% yield. ESI-MS: *m/z* 473.2 $[M+Na]^+$.

4.1.21. Hydrogenation of nitroarenes.

For a typical run, a solution of 6-(4-amino-3-nitrophenyl)-3-(2-morpholino-2-oxoethyl)quinazolin-4(3*H*)-one (1.975 g, 5 mmol) and Pd/C 0.118 g (10% on Carbon, wetted with ca.55% water) in 30 mL MeOH was stirred at ambient temperature for 15 min, then the hydrazine hydrate (2.50 g, 50 mmol) was added at

this temperature and was stirred for another 15 min. The reaction mixture was heated to reflux and stirred about 2 h. After the desired reaction time, the mixture was filtrated with Celite, the remaining hydrazine hydrate was removed under reduced pressure to offered corresponding 6-(3, 4-diaminophenyl)-3-(2-morpholino-2-oxoethyl)quinazolin-4(3*H*)-one **14a** which was used in the next step directly without another purification.

Compounds **14b-i** were synthesized according to the procedure described in **14a**.

*4.1.22. Preparation of 6-(2-amino-1H-benzo[d]imidazol-6-yl)-3-(2-morpholino-2-oxoethyl)quinazolin-4(3H)-one (**15a**).*

The **14a** (1.14 g, 3 mmol) was dissolved in a 1:1 mixture of methanol (15 mL) and water (15 mL). The reaction mixture was treated with CNBr (0.95 g, 9 mmol) and heated at 60 °C for 2 h. After cooling to room temperature, methanol was removed under reduced pressure and the remaining reaction mixture was basified with 1M NaOH aq. to pH=8, then extracted with *n*-butanol (3×30 mL). The combined organic fractions were washed with water (2×50 mL), brine (2×50 mL), dried over $MgSO_4$ and the solvent was removed under reduced pressure, the residue was purified through a column chromatography on silica with dichloromethane/methanol/ammonia system to give the pure title compound **15a**, as white solid, 65.0% yield. ESI-MS (Neg.): *m/z* 403.1 $[M-H]^-$.

Compounds **15b-h** were synthesized according to the procedure described in **15a**.

*4.1.23. 6-(2-amino-1H-benzo[d]imidazol-6-yl)-3-(2-(piperidin-1-yl)ethyl)quinazolin-4(3H)-one (**15b**).*

White solid keeping under argon, 60.2% yield. ESI-MS (Neg.): *m/z* 387.2 $[M-H]^-$.

*4.1.24. 6-(2-amino-1H-benzo[d]imidazol-6-yl)-3-methylquinazolin-4(3H)-one (**15c**).*

White solid keeping under argon, 63.2% yield. ESI-MS (Neg.): *m/z* 290.1 $[M-H]^-$.

*4.1.25. 6-(2-amino-1H-benzo[d]imidazol-6-yl)-3-(2-morpholinoethyl)quinazolin-4(3H)-one (**15d**).*

White solid keeping under argon, 63.1% yield. ESI-MS (Neg.): *m/z* 389.1 $[M-H]^-$.

*4.1.26. 6-(2-amino-1H-benzo[d]imidazol-6-yl)-3-butylquinazolin-4(3H)-one (**15e**).*

White solid keeping under argon, 64.1% yield. ESI-MS (Neg.): *m/z* 332.1 $[M-H]^-$.

*4.1.27. 3-(2-(1H-indol-3-yl)ethyl)-6-(2-amino-1H-benzo[d]imidazol-6-yl)quinazolin-4(3H)-one (**15f**).*

White solid keeping under argon, 59.6% yield. ESI-MS (Neg.): *m/z* 419.1 $[M-H]^-$.

*4.1.28 6-(2-amino-1H-benzo[d]imidazol-6-yl)-3-(3-morpholinopropyl)quinazolin-4(3H)-one (**15g**).*

White solid keeping under argon, 63.7% yield. ESI-MS (Neg.): *m/z* 403.2 $[M-H]^-$.

*4.1.29. 6-(2-amino-1H-benzo[d]imidazol-6-yl)-3-methyl-2-(morpholinomethyl)-quinazolin-4(3H)-one (**15h**).*

White solid keeping under argon, 61.5% yield. ESI-MS (Neg.): *m/z* 389.1 $[M-H]^-$.

*4.1.30. 6-(2-amino-1H-benzo[d]imidazol-6-yl)-3-methyl-2-((4-propionylpiperazin-1-yl)methyl)quinazolin-4(3H)-one (**15i**).*

White solid keeping under argon, 59.5% yield. ESI-MS (Neg.): *m/z* 444.2 $[M-H]^-$.

*4.1.31. N-(6-(3-(2-morpholino-2-oxoethyl)-4-oxo-3,4-dihydroquinazolin-6-yl)-1H-benzo[d]imidazol-2-yl)ethanesulfonamide (**16a**).*

A solution of **15a** (0.404 g, 1 mmol) and triethylamine (0.152 g, 1.5 mmol) in anhydrous tetrahydrofuran (THF, 20 mL) was stirred for 45 min. Subsequently, a solution of ethanesulfonyl chloride (0.128 g, 1 mmol) in THF (5 mL) was added drop wisely to the reaction mixture under ice cold conditions using a dropping funnel and the contents were stirred further for 2 h at ambient temperature. Completion of the reaction was monitored by TLC. The slurry was pulled into saturated salt water 50 mL and extracted with dichloromethane (50 mL×3), the combined organic fractions were washed with saturated $NaHCO_3$ aqueous solution three times, dried over $MgSO_4$ and the solvent was removed under reduced pressure to obtain a solid residue which was purified through a column chromatography on silica with dichloromethane /methanol to afford **16a,** as a white solid (0.274 g, 0.552 mmol, 55.2% yield), mp 237-239 ℃. ^{1}H NMR (600 MHz, DMSO-d_6) δ 8.31 (d, J = 2.3 Hz, 1H), 8.26 (s, 1H), 8.15 (dd, J = 8.5, 2.3 Hz, 1H), 7.82 (d, J = 1.8 Hz, 1H), 7.79 (d, J = 8.5 Hz, 1H), 7.59 (dd, J = 8.2, 1.8 Hz, 1H), 7.37 (d, J = 8.2 Hz, 1H), 7.09 (s, 2H), 4.98 (s, 2H), 3.78 (q, J = 7.2 Hz, 2H), 3.69 (t, J = 4.7 Hz, 2H), 3.64-3.57 (m, 4H), 3.48 (t, J = 4.9 Hz, 2H), 1.22 (t, J = 7.2 Hz, 3H). ^{13}C NMR (151 MHz, DMSO-d_6) δ 165.68, 160.72, 153.68, 148.74, 147.34, 143.14, 139.81, 133.46, 132.29, 131.79, 128.45, 124.00, 123.32, 122.27, 116.87, 110.56, 66.48, 66.44, 48.53, 47.10, 45.24, 42.54, 8.00. HRMS (ESI): calcd. for $C_{23}H_{25}O_5N_6S$ $[M+H]^+$ *m/z* 497.1602, found 497.1589; $C_{23}H_{24}O_5N_6NaS$ $[M+Na]^+$ *m/z* 519.1421, found 519.1414.

Compounds **16b-t** were synthesized according to the procedure described in **16a**.

4.1.32. N-(6-(3-(2-morpholino-2-oxoethyl)-4-oxo-3,4-dihydroquinazolin-6-yl)-1H-

*benzo[d]imidazol-2-yl)propionamide (**16b**).*

White solid, 51.7% yield, mp 289-291□. ^{1}H NMR (600 MHz, DMSO-d_6) δ 12.16 (s, 1H), 11.58 (s, 1H), 8.33 (s, 1H), 8.26 (s, 1H), 8.20 – 8.14 (1H), 7.84 – 7.78 (2H), 7.59 – 7.51 (2H), 4.98 (s, 2H), 3.69 (bs, 2H), 3.60 (bs, 4H), 3.48 (bs, 2H), 2.47 (q, J =7.3 Hz, 2H), 1.22 (t, J =7.03 Hz, 2H). ^{13}C NMR (151 MHz, DMSO-d_6) δ 165.72, 165.65, 160.76, 160.63, 149.33, 148.62, 148.15, 147.19, 137.75, 133.46, 128.74, 124.13, 122.38, 66.47, 66.43, 47.13, 45.23, 42.54, 29.23, 9.64. HRMS (ESI): calcd. for $C_{24}H_{25}O_4N_6$ $[M+H]^+$ *m/z* 461.1932, found 461.1919; $C_{24}H_{24}O_4NaN_6$ $[M+Na]^+$ *m/z* 483.1751, found 483.1740.

*4.1.33. N-(6-(3-methyl-4-oxo-3,4-dihydroquinazolin-6-yl)-1H-benzo[d]imidazol-2-yl)propionamide (**16c**).*

White solid, 53.5% yield, mp 248-250 □. ^{1}H NMR (600 MHz, DMSO-d_6) δ 12.16 (s, 1H), 11.58 (s, 1H), 8.37 (s, 1H), 8.34 (d, J = 2.2 Hz, 1H), 8.12 (d, J = 8.8 Hz, 1H), 7.81 (bs, 1H), 7.74 (d, J = 8.4 Hz, 1H), 7.55 (d, J = 8.3 Hz, 1H), 7.49 (d, J = 8.3 Hz, 1H), 3.53 (s, 3H), 2.47 (q, J = 7.6 Hz, 2H), 1.14 (t, J = 7.5 Hz, 3H). ^{13}C NMR (151 MHz, DMSO) δ 173.81, 161.25, 148.53, 148.05, 147.27, 140.31, 133.16, 132.60, 128.27, 123.16, 122.23, 120.72, 34.06, 29.23, 9.64. HRMS (ESI): calcd. for $C_{19}H_{18}O_2N_5$ $[M+H]^+$ *m/z* 348.1455, found 348.1451; $C_{19}H_{17}O_2NaN_5$ $[M+Na]^+$ *m/z* 370.1274, found 370.1262.

*4.1.34. N-(6-(3-methyl-4-oxo-3,4-dihydroquinazolin-6-yl)-1H-benzo[d]imidazol-2-yl)ethanesulfonamide (**16d**).*

White solid, 53.5% yield, mp 230-232 □. ^{1}H NMR (600 MHz, DMSO-d_6) δ 8.38

(s, 1H), 8.34 (d, *J* = 2.3 Hz, 1H), 8.13 (dd, *J* = 8.5, 2.3 Hz, 1H), 7.74 (d, *J* = 8.4 Hz, 1H), 7.62 – 7.57 (m, 2H), 7.43 (dd, *J* = 8.3, 1.9 Hz, 1H), 7.09 (s, 2H), 3.72 (q, *J* = 7.3 Hz, 2H), 3.53 (s, 3H), 1.21 (t, *J* = 7.3 Hz, 3H). ^{13}C NMR (151 MHz, DMSO-d_6) δ 161.20, 153.66, 148.67, 147.44, 143.09, 139.64, 133.15, 132.28, 131.86, 128.37, 124.00, 123.12, 122.26, 116.85, 110.53, 48.51, 34.07, 8.01. HRMS (ESI): calcd. for $C_{18}H_{18}O_3N_5S$ $[M+H]^+$ *m/z* 384.1125, found 348.1115.

*4.1.35. N-(6-(3-methyl-2-(morpholinomethyl)-4-oxo-3,4-dihydroquinazolin-6-yl)-1H-benzo[d]imidazol-2-yl)propionamide (**16e**).*

White solid, 51.9% yield, mp 219-221 □, ^{1}H NMR (600 MHz, DMSO-d_6) δ 12.14 (s, 1H), 11.60 (s, 1H), 8.32 (d, *J* = 2.1 Hz, 1H), 8.10 (d, *J* = 8.6 Hz, 1H), 7.80 (s, 1H), 7.72 (d, *J* = 8.5 Hz, 1H), 7.55 (bs, 1H), 7.48 (dd, *J* = 8.3, 1.8 Hz, 1H), 3.72 (s, 3H), 3.67 (s, 2H), 3.58 (t, *J* = 4.6 Hz, 4H), 3.35 (s, 4H), 2.47 (q, *J* = 7.6 Hz, 1H), 1.14 (t, *J* = 7.5 Hz, 3H). ^{13}C NMR (151 MHz, DMSO-d_6) δ 173.81, 162.25, 153.75, 148.05, 145.65, 140.25, 128.13, 123.45, 120.98, 120.79, 66.65, 62.98, 53.51, 40.51, 30.74, 29.23, 27.35, 9.64. HRMS (ESI): calcd. for $C_{24}H_{27}O_3N_6$ $[M+H]^+$ *m/z* 447.2139, found 447.2133; $C_{24}H_{26}O_3NaN_6$ $[M+Na]^+$ *m/z* 469.1959, found 469.1949.

*4.1.36. N-(6-(3-methyl-4-oxo-2-((4-propionylpiperazin-1-yl)methyl)-3,4-dihydroquinazolin-6-yl)-1H-benzo[d]imidazol-2-yl)propionamide (**16f**).*

White solid, 49.7% yield, mp 224-226 □, ^{1}H NMR (600 MHz, DMSO-d_6) δ 11.97 (s, 1H), 11.41 (s, 1H), 8.35 (d, *J* = 2.1 Hz, 1H), 8.13-8.09 (m, 1H), 7.81 (s, 1H), 7.73 (d, *J* = 8.4 Hz, 1H), 7.59-7.53 (m, 1H), 7.49 (d, *J* = 8.0 Hz, 1H), 3.75 (s, 3H), 3.48 (bs, 4H), 3.20 (s, 2H), 2.54 (bs, 4H), 2.48 (q, *J* = 7.5 Hz, 2H), 2.31 (q, *J* =7.4 Hz,

2H), 1.17 (t, *J* = 7.5 Hz, 3H), 1.01 (d, *J* = 7.4 Hz, 3H). ^{13}C NMR (151 MHz, DMSO-d_6) δ 174.03, 171.98, 162.30, 148.25, 145.80, 140.51, 133.14, 132.93, 128.06, 120.97, 53.03, 49.05, 48.52, 30.70, 29.39, 25.96, 18.34, 12.37, 9.67, 9.47. HRMS (ESI): calcd. for $C_{27}H_{32}O_3N_7$ $[M+H]^+$ *m/z* 502.2561, found 502.2556; $C_{27}H_{31}O_3NaN_7$ $[M+Na]^+$ *m/z* 524.2381, found 524.2374.

*4.1.37. N-(6-(3-(2-morpholinoethyl)-4-oxo-3,4-dihydroquinazolin-6-yl)-1H-benzo[d]imidazol-2-yl)ethanesulfonamide (**16g**).*

White solid, 51.6% yield, mp 210-212 □, ^{1}H NMR (600 MHz, DMSO-d_6) δ 8.34 (s, 1H), 8.33 (d, *J* = 2.2 Hz, 1H), 8.13 (dd, *J* = 8.5, 2.2 Hz, 1H), 7.81 (d, *J* = 1.5 Hz, 1H), 7.76 (d, *J* = 8.5 Hz, 1H), 7.59 (dd, *J* = 8.2, 1.7 Hz, 1H), 7.36 (d, *J* = 8.2 Hz, 1H), 7.08 (s, 2H), 4.12 (t, *J* = 6.1 Hz, 2H), 3.78 (q, *J* = 7.3 Hz, 2H), 3.53 (t, *J* = 4.6 Hz, 4H), 2.63 (t, *J* = 6.1 Hz, 2H), 2.45 (s, 4H), 1.21 (t, *J* = 7.3 Hz, 4H). ^{13}C NMR (151 MHz, DMSO-d_6) δ 160.70, 153.67, 148.63, 147.28, 143.10, 139.63, 133.29, 132.28, 131.85, 128.37, 123.99, 123.35, 122.32, 116.85, 110.54, 66.71, 56.80, 53.67, 48.51, 43.11, 8.01. HRMS (ESI): calcd. for $C_{23}H_{27}O_4N_6S$ $[M+H]^+$ *m/z* 483.1809, found 483.1801; $C_{23}H_{26}O_4NaN_6S$ $[M+Na]^+$ *m/z* 505.1628 , found 505.1615.

*4.1.38. N-(6-(3-(2-morpholinoethyl)-4-oxo-3,4-dihydroquinazolin-6-yl)-1H-benzo[d]imidazol-2-yl)propionamide (**16h**).*

White solid, 53.3% yield, mp 237-239 □, ^{1}H NMR (600 MHz, DMSO-d_6) δ 11.34 (s, 2H), 8.40 (t, *J* = 2.3 Hz, 1H), 8.27 (d, *J* = 2.4 Hz, 1H), 8.10 (dd, *J* = 8.4, 2.5 Hz, 1H), 7.82 (s, 1H), 7.74 (d, *J* = 8.4 Hz, 1H), 7.56 (d, *J* = 8.1 Hz, 1H), 7.49 (dd, *J* = 8.5, 2.2 Hz, 1H), 4.14 (t, *J* = 6.4 Hz, 2H), 3.59-3.56 (m, 4H), 2.85 (bs, 4H), 2.73 (t, *J*

= 6.3 Hz, 2H), 2.51 (m, 2H), 1.20 (t, *J* = 7.4 Hz, 3H). ^{13}C NMR (151 MHz, DMSO-d_6) δ 174.11, 160.90, 148.37, 148.01, 147.31, 140.66, 133.11, 132.99, 128.13, 123.63, 122.52, 120.82, 66.79, 56.92, 53.81, 43.55, 29.44, 9.41. HRMS (ESI): calcd. for $C_{24}H_{27}O_3N_6$ $[M+H]^+$ *m/z* 447.2139, found 447.2132; $C_{24}H_{26}O_3NaN_6$ $[M+Na]^+$ *m/z* 469.1959 , found 469.1948.

*4.1.39. N-(6-(4-oxo-3-(2-(piperidin-1-yl)ethyl)-3,4-dihydroquinazolin-6-yl)-1H-benzo[d]imidazol-2-yl)propionamide (**16i**).*

White solid, 52.9% yield, mp 245-247 □, ^{1}H NMR (600 MHz, DMSO-d_6) δ 11.45 (bs, 1H), 10.39 (s, 1H), 8.31 (s, 1H), 8.18 (d, *J* = 2.3 Hz, 1H), 8.00 (dd, *J* = 8.5, 2.3 Hz, 1H), 7.64 (s, 1H), 7.61 (d, *J* = 8.4 Hz, 1H), 7.39 (d, *J* = 8.3 Hz, 1H), 7.33 (dd, *J* = 8.3, 1.8 Hz, 1H), 4.30 (t, *J* = 6.7 Hz, 2H), 3.44 – 3.35 (m, 2H), 3.20 (bs, 4H), 2.80 (bs, 2H), 2.32 (q, *J* = 7.5 Hz, 2H), 1.64 (bs, 4H), 0.97 (t, *J* = 7.5 Hz, 3H). ^{13}C NMR (151 MHz, DMSO-d_6) δ 173.86, 161.26, 148.06, 147.83, 147.02, 140.56, 133.53, 132.41, 128.38, 123.62, 122.38, 120.80, 54.49, 52.86, 41.11, 29.24, 22.82, 21.77, 9.64. HRMS (ESI): calcd. for $C_{25}H_{29}O_2N_6$ $[M+H]^+$ *m/z* 445.2347, found 445.2341.

4.1.40. N-(6-(3-(2-morpholinoethyl)-4-oxo-3,4-dihydroquinazolin-6-yl)-1H-benzo[d]imidazol-2-yl)pentanamide (***16j***).

White solid, 55.6% yield, mp 238-240 □, ^{1}H NMR (600 MHz, DMSO-d_6) δ 12.17 (s, 1H), 11.59 (s, 1H), 8.35 (s, 1H), 8.32 (s, 1H), 8.13 (bs, 1H), 7.80 (m, 1H), 7.75 (d, *J* = 8.4 Hz, 1H), 7.59 – 7.52 (m, 1H), 7.49 (d, *J* = 7.9 Hz, 1H), 4.12 (t, *J* = 6.1 Hz, 2H), 3.53 (t, *J* = 4.6 Hz, 4H), 2.63 (t, *J* = 5.9 Hz, 2H), 2.48 – 2.43 (6H), 2.31-2.27 (bs, 4H), 1.63 (p, *J* = 5.9 Hz, 2H), 1.39-1.32 (m, 2H), 0.91 (t, *J* = 7.4 Hz, 3H). ^{13}C

NMR (151 MHz, DMSO-d_6) δ 173.14, 160.75, 148.48, 148.02, 147.12, 140.35, 133.22, 128.28, 123.36, 122.30, 121.02, 66.71, 56.86, 53.68, 43.08, 35.62, 27.32, 22.19, 14.17. HRMS (ESI): calcd. for $C_{26}H_{31}O_3N_6$ $[M+H]^+$ *m/z* 475.2452, found 475.2448; $C_{26}H_{30}O_3NaN_6$ $[M+Na]^+$ *m/z* 497.2272, found 497.2260.

*4.1.41. N-(6-(3-(3-morpholinopropyl)-4-oxo-3,4-dihydroquinazolin-6-yl)-1H-benzo[d]imidazol-2-yl)propionamide (**16k**).*

White solid, 53.6% yield, mp 243-245℃, ^{1}H NMR (600 MHz, DMSO-d_6) δ 12.15 (s, 1H), 11.58 (s, 1H), 8.38 (s, 1H), 8.35 (s, 1H), 8.13 (bs, 1H), 7.83 (1H), 7.75 (d, *J* = 8.4 Hz, 1H), 7.54 (1H), 7.50 (d, *J* = 8.3 Hz, 1H), 4.05 (t, *J* = 6.9 Hz, 2H), 3.48 (t, *J* = 4.6 Hz, 4H), 2.48 (q, *J* = 7.7 Hz, 2H), 2.33 (t, *J* = 6.6 Hz, 2H), 2.30 (bs, 4H), 1.89 (p, *J* = 6.7 Hz, 2H), 1.14 (t, *J* = 7.5 Hz, 3H); ^{13}C NMR (151 MHz, DMSO-d_6) δ 173.81, 160.91, 148.46, 148.06, 147.18, 140.32, 133.31, 133.13, 128.25, 123.36, 122.40, 120.94, 117.83, 66.56, 55.58, 53.54, 45.29, 29.23, 25.05, 9.64. HRMS (ESI): calcd. for $C_{25}H_{29}O_3N_6$ $[M+H]^+$ *m/z* 461.2296, found 461.2289; $C_{25}H_{28}O_3NaN_6$ $[M+Na]^+$ *m/z* 483.2115, found 483.2104.

*4.1.42. N-(6-(3-butyl-4-oxo-3,4-dihydroquinazolin-6-yl)-1H-benzo[d]imidazol-2-yl)propionamide (**16l**).*

White solid, 54.1% yield, mp 286-288 ℃, ^{1}H NMR (600 MHz, DMSO-d_6) δ 12.17 (s, 1H), 11.58 (s, 1H), 8.40 (s, 1H), 8.35 (d, *J* = 2.0 Hz, 1H), 8.14 (d, *J* = 8.3 Hz, 1H), 7.81 (s, 1H), 7.75 (d, *J* = 8.5 Hz, 1H), 7.55 (d, *J* = 8.2 Hz, 1H), 7.50 (dd, *J* = 8.3, 1.4 Hz, 1H), 4.01 (t, *J* = 7.3 Hz, 2H), 2.48 (q, *J* = 7.5 Hz, 2H), 1.71 (m, *J* = 7.5 Hz, 2H), 1.34 (h, *J* = 7.5 Hz, 2H), 1.14 (t, *J* = 7.5 Hz, 3H), 0.93 (t, *J* = 7.4 Hz, 3H). ^{13}C

NMR (151 MHz, DMSO-d_6) δ 173.81, 160.74, 148.16, 148.04, 147.12, 140.41, 133.28, 128.30, 123.38, 122.35, 120.87, 120.78, 110.60, 46.18, 31.23, 29.23, 19.78, 14.03, 9.64. HRMS (ESI): calcd. for $C_{22}H_{24}O_2N_5$ $[M+H]^+$ *m/z* 390.1925, found 390.1914; $C_{22}H_{23}O_2NaN_5$ $[M+Na]^+$ *m/z* 412.1744, found 412.1732.

*4.1.43. methyl (6-(3-(2-morpholinoethyl)-4-oxo-3,4-dihydroquinazolin-6-yl)-1H-benzo[d]imidazol-2-yl)carbamate (**16m**).*

White solid, 45.6% yield, mp 294-296 □, ^{1}H NMR (600 MHz, DMSO-d_6) δ 11.73 (bs, 2H), 8.35 (d, *J* = 2.3 Hz, 1H), 8.33 (s, 1H), 8.13 (dd, *J* = 8.5, 2.3 Hz, 1H), 7.79-7.73 (m, 2H), 7.52 (d, *J* = 8.2 Hz, 1H), 7.49 (dd, *J* = 8.3, 1.8 Hz, 1H), 4.12 (t, *J* = 6.1 Hz, 2H), 3.78 (s, 3H), 3.54 (t, *J* = 4.6 Hz, 4H), 2.64 (t, *J* = 6.1 Hz, 2H), 2.46 (s, 4H). ^{13}C NMR (151 MHz, DMSO-d_6) δ 160.74, 155.39, 148.77, 148.52, 147.15, 140.26, 133.30, 132.52, 128.30, 123.40, 122.31, 120.77, 66.72, 56.86, 53.69, 52.97, 49.07, 43.09. HRMS (ESI): calcd. for $C_{23}H_{25}O_4N_6$ $[M+H]^+$ *m/z* 449.1932, found 449.1924; $C_{23}H_{24}O_4NaN_6$ $[M+Na]^+$ *m/z* 471.1751, found 471.1740.

*4.1.44. 1,1-dimethyl-3-(6-(3-(2-morpholinoethyl)-4-oxo-3,4-dihydroquinazolin-6-yl)-1H-benzo[d] imidazol -2-yl)urea (**16n**).*

White solid, 46.9% yield, mp 229-231□, ^{1}H NMR (600 MHz, DMSO-d_6) δ 8.32 (s, 1H), 8.31 (d, *J* = 2.2 Hz, 1H), 8.12 (dd, *J* = 8.5, 2.3 Hz, 1H), 7.73 (d, *J* = 8.4 Hz, 1H), 7.45 (dd, *J* = 8.2, 1.8 Hz, 1H), 7.43 (d, *J* = 1.8 Hz, 1H), 7.30 (d, *J* = 8.1 Hz, 1H), 6.82 (s, 2H), 4.12 (t, *J* = 6.1 Hz, 2H), 3.54 (t, *J* = 4.4 Hz, 4H), 3.03 (s, 6H), 2.63 (t, *J* = 6.1 Hz, 2H), 2.45 (bs, 4H). ^{13}C NMR (151 MHz, DMSO-d_6) δ 160.73, 154.39, 152.03, 148.43, 147.03, 143.63, 140.04, 133.42, 133.25, 130.69, 128.22, 123.15, 122.28,

121.82, 116.14, 108.37, 66.70, 56.85, 53.68, 43.08, 37.92. HRMS (ESI): calcd. for $C_{24}H_{28}O_3N_7$ $[M+H]^+$ *m/z* 462.2284, found 462.2241; $C_{24}H_{27}O_3NaN_7$ $[M+Na]^+$ *m/z* 484.2608, found 484.2053.

*4.1.45. 1,1-diethyl-3-(6-(3-(2-morpholinoethyl)-4-oxo-3,4-dihydroquinazolin-6-yl)-1H-benzo[d]imidazol-2-yl)urea (**16o**).*

White solid, 45.2% yield, mp 230-232□, ^{1}H NMR (600 MHz, DMSO-d_6) δ 8.34 (d, *J* = 2.3 Hz, 1H), 8.33 (s, 1H), 8.14 (dd, *J* = 8.5, 2.2 Hz, 1H), 7.74 (d, *J* = 8.5 Hz, 1H), 7.55 (d, *J* = 1.5 Hz, 1H), 7.13 (d, *J* = 8.1 Hz, 1H), 6.77 (s, 2H), 4.12 (t, *J* = 6.0 Hz, 2H), 3.54 (t, *J* = 4.1 Hz , 4H), 3.34 (4H), 2.64 (t, *J* = 5.9 Hz, 2H), 2.46 (bs, 4H), 1.17 (t, *J* = 7.1 Hz, 6H). ^{13}C NMR (151 MHz, DMSO-d_6) *δ* 160.71, 154.51, 151.38, 148.48, 147.06, 143.56, 139.96, 133.48, 133.13, 130.75, 128.31, 123.06, 122.31, 121.86, 116.26, 107.34, 66.66, 56.81, 53.65, 43.05, 42.86, 13.98. HRMS (ESI): calcd. for $C_{26}H_{32}O_3N_7$ $[M+H]^+$ *m/z* 490.2561, found 490.2553; $C_{26}H_{31}O_3NaN_7$ $[M+Na]^+$ *m/z* 512.2381, found 512.2372.

4.1.46. N-(6-(3-(2-morpholinoethyl)-4-oxo-3,4-dihydroquinazolin-6-yl)-1H-benzo[d]imidazol-2-yl)cyclopropanecarboxamide (***16p***).

White solid, 54.2% yield, mp 239-241 ℃, ^{1}H NMR (600 MHz, DMSO-d_6) *δ* 12.12 (s, 1H), 11.93 (s, 1H), 8.35 (d, *J* = 2.2 Hz, 1H), 8.33 (s, 1H), 8.14 (s, 1H), 7.80 (s, 1H), 7.75 (d, *J* = 8.5 Hz, 1H), 7.55 (d, *J* = 8.3 Hz, 1H), 7.49 (dd, *J* = 8.3, 1.8 Hz, 1H), 4.12 (t, *J* = 6.1 Hz, 2H), 3.54 (t, *J* = 4.6 Hz, 4H), 2.64 (s, 2H), 2.46 (s, 4H), 2.03-1.98 (m, 1H), 0.94 (d, *J* = 5.4 Hz, 4H). ^{13}C NMR (151 MHz, DMSO-d_6) *δ* 173.52, 160.76, 148.48, 147.99, 147.12, 140.37, 133.40, 128.28, 123.40, 122.31,

66.70, 56.84, 53.67, 49.07, 43.06, 14.38, 8.76. HRMS (ESI): calcd. for $C_{25}H_{27}O_3N_6$ $[M+H]^+$ *m/z* 459.2139, found 459.2132; $C_{25}H_{26}O_3NaN_6$ $[M+Na]^+$ *m/z* 481.1959, found 481.1950.

4.1.47. N-(6-(3-(2-morpholinoethyl)-4-oxo-3,4-dihydroquinazolin-6-yl)-1H-benzo[d]imidazol-2-yl)cyclohexanecarboxamide (***16q***).

White solid, 55.6% yield, mp 242-244 □, ^{1}H NMR (600 MHz, DMSO-d_6) δ 12.19 (s, 1H), 11.55 (s, 1H), 8.35 (s, 1H), 8.32 (s, 1H), 8.13 (s, 1H), 7.80 (s, 1H), 7.75 (d, *J* = 8.5 Hz, 1H), 7.54 (s, 1H), 7.49 (dd, *J* = 8.2, 1.8 Hz, 1H), 4.11 (t, *J* = 6.1 Hz, 2H), 3.54 (t, *J* = 4.6 Hz, 4H), 2.63 (t, *J* = 6.1 Hz, 2H), 2.45 (t, *J* = 4.6 Hz, 1H), 2.46 (bs, 4H), 1.88 (dd, *J* = 12.8, 3.7 Hz, 2H), 1.78 (dt, *J* = 12.9, 3.4 Hz, 2H), 1.68 – 1.62 (m, 1H) 1.47 (qd, *J* = 12.4, 3.4 Hz, 2H), 1.33-1.19 (m, 4H). ^{13}C NMR (151 MHz, DMSO-d_6) δ 176.04, 160.74, 148.48, 148.17, 147.12, 140.30, 133.98, 133.17, 128.27, 123.42, 122.30, 121.02, 120.57, 117.84, 112.39, 109.90, 66.72, 56.87, 53.68, 44.23, 43.08, 29.30, 25.78, 25.50. HRMS (ESI): calcd. for $C_{28}H_{33}O_3N_6$ $[M+H]^+$ *m/z* 501.2609, found 501.2603; $C_{28}H_{32}O_3NaN_6$ $[M+Na]^+$ *m/z* 523.2428, found 523.2421.

4.1.48. N-(6-(3-(2-morpholinoethyl)-4-oxo-3,4-dihydroquinazolin-6-yl)-1H-benzo[d]imidazol-2-yl)benzamide (***16r***).

White solid, 60.4% yield, mp 194-196 □, ^{1}H NMR (600 MHz, DMSO-d_6) δ 12.35 (s, 2H), 8.37 (d, *J* = 2.2 Hz, 1H), 8.34 (s, 1H), 8.17 – 8.14 (m, 3H), 7.84 (s, 1H), 7.77 (d, *J* = 8.5 Hz, 1H), 7.65-7.61 (m, 1H), 7.60 (d, *J* = 8.3 Hz, 1H), 7.58-7.54 (m, 3H), 4.13 (t, *J* = 6.1 Hz, 2H), 3.54 (t, *J* = 4.6 Hz, 4H), 2.64 (t, *J* = 6.1 Hz, 2H), 2.46 (bs, 4H). ^{13}C NMR (151 MHz, DMSO-d_6) δ 160.78, 149.70, 148.60, 147.24, 140.11,

133.38, 133.08, 132.75, 128.94, 128.77, 128.35, 123.51, 122.32, 121.35, 66.72, 56.85, 53.68, 43.11. HRMS (ESI): calcd. for $C_{28}H_{27}O_3N_6$ $[M+H]^+$ *m/z* 495.2139, found 495.2135; $C_{28}H_{26}O_3NaN_6$ $[M+Na]^+$ *m/z* 517.1959, found 517.1950.

4.1.49. N-(6-(3-(2-morpholinoethyl)-4-oxo-3,4-dihydroquinazolin-6-yl)-1H-benzo[d]imidazol-2-yl)morpholine-4-carboxamide (***16s***).

White solid, 44.7% yield, mp 134-136 □, ^{1}H NMR (600 MHz, methanol-d_4) δ 8.24 (d, *J* = 1.9 Hz, 1H), 8.22 (s, 1H), 7.95 (dd, *J* = 8.5, 2.0 Hz, 1H), 7.60 (d, *J* = 8.5 Hz, 1H), 7.44 (dd, *J* = 1.9 Hz, 1H), 7.40-7.38 (dd, *J* = 8.5, 2.0 Hz, 1H), 7.29 (d, *J* = 8.2 Hz, 1H), 4.16 (t, *J* = 6.1 Hz, 2H), 3.81 – 3.73 (m, 4H), 3.68 (t, *J* =4.2 Hz, 4H), 3.63 (t, *J* = 4.2 Hz, 4H), 2.80 (t, *J* = 6.1 Hz, 2H), 2.63 (bs, 4H). ^{13}C NMR (151 MHz, MeOD) δ 161.27, 154.21, 151.17, 147.61, 146.34, 140.25, 139.97, 132.86, 132.43, 132.38, 131.58, 129.70, 127.02, 124.88, 123.23, 122.56, 121.67, 115.24, 108.52, 66.25, 56.35, 53.23, 46.52, 42.85, 7.86. HRMS (ESI): calcd. for $C_{26}H_{30}O_4N_7$ $[M+H]^+$ *m/z* 504.2354, found 504.2348; $C_{26}H_{29}O_4NaN_7$ $[M+Na]^+$ *m/z* 526.2173, found 526.2162.

*4.1.50. N-(6-(3-(2-(1H-indol-3-yl)ethyl)-4-oxo-3,4-dihydroquinazolin-6-yl)-1H-benzo[d]imidazol-2-yl)propionamide (**16t**).*

White solid, 48.8% yield, mp 292-294 □, ^{1}H NMR (600 MHz, DMSO-d_6) δ 12.16 (s, 1H), 11.58 (s, 1H), 10.87 (s, 1H), 8.41 (s, 1H), 8.17-8.10 (m, 1H), 8.09 (s, 1H), 7.85 – 7.80 (1H), 7.70 (d, *J* = 8.4 Hz, 1H), 7.65 (d, *J* = 7.8 Hz, 1H), 7.58 – 7.48 (m, 2H), 7.36 (d, *J* = 8.2 Hz, 1H), 7.15 (s, 1H), 7.09 (t, *J* = 7.7 Hz, 1H), 6.99 (t, *J* = 7.5 Hz, 1H), 4.29 (t, *J* = 7.5 Hz, 2H), 3.17 (t, *J* = 7.6 Hz, 2H), 2.47 (q, *J* = 6.9 Hz, 2H),

1.14 (t, J = 7.6 Hz, 3H). ^{13}C NMR (151 MHz, DMSO-d_6) δ 173.83, 160.80, 148.08, 147.96, 147.11, 140.37, 136.77, 133.38, 133.13, 128.30, 128.26, 127.50, 123.86, 123.46, 123.37, 122.40, 121.57, 118.92, 118.76, 111.96, 110.67, 47.26, 29.24, 24.97, 9.65. HRMS (ESI): calcd. for $C_{28}H_{25}O_2N_6$ $[M+H]^+$ *m/z* 477.2034, found 477.2024; $C_{28}H_{24}O_2NaN_6$ $[M+Na]^+$ *m/z* 499.1853, found 499.1841.

4.2. Biological evaluation

All compounds were dissolved in DMSO to make a 20 mM stock solution. DMEM (Dulbecco's modified Eagle's) medium was purchased from Gibco Life Technologies. Methylthiazolyltetrazolium (MTT) was purchased from Sigma (St Louis, MO, USA). Antibodies against cleaved-PARP, cleaved-caspase 3, cleaved-caspase 9, phosphor-Aurroa A/B/C kinase and phosphor-Histone H3 were purchased from Cell Signaling Technology (CST, Danvers, MA, USA). Antibodies against histone H3, Aurora A kinase and GAPDH were were purchased from Proteintech (Boston, MA, USA).

4.2.1. Aurora kinase assay

The effect of **16h** on Aurora A and Aurora B kinases were assayed using the homogeneous time-resolved fluorescence (HTRF) KinEASE STK2 kit from Cisbio (France) according to the protocol of HTRF KinEASE-TK kit. For both enzymes, the reactions were run for 30 min at room temperature and stopped by the addition of 10 μL of detection buffer containing EDTA, antiphospho-Ser/Thr antibody labeled with europium cryptate, and XL-665 conjugated streptavidin (62.5 nM final concentration). After incubation at room temperature for 1 h, fluorescence was measured at 620 nm

(europium cryptate) and 665 nm (XL-665) after excitation at 317 nm. The ratio of fluorescence (665 nm/620 nm) was calculated for each well, and the results were expressed as follows: specific signal = ratio (sample) - ratio (negative control), where ratio = 665/620 nm×10^4. Compounds were measured in 3-fold serial dilutions at 10 different concentrations, covering the concentration range from no to full inhibition. Each concentration was measured in duplicates, and two independent determinations were made for each IC_{50} value. IC_{50} curves were generated using a four-parameter logistic model. The inhibitory activity was represented as the relative percentage inhibition of the positive control staurosporine.

4.2.2. Cell culture

The MDA-MB-231, PC3 and SH-SY5Y cells were obtained from Cell Bank of the Chinese Academy of Sciences (Shanghai, China) and cultured according to their recommendations. In brief, the cells were cells were cultured with DMEM medium containing 10% FBS and 10% penicillin-streptomycin and incubated at 37 □ in a humidified incubator with 5% CO_2.

4.2.3. Cytotoxicity assay

Cytotoxicity assay was measured by MTT assays previously described [42-44]. Cells were seeded in 96-well plates (5×10^3 cells per well) and cultured with different concentrations of synthesized compounds.

4.2.4. Colony formatting

MDA-MB-231 cells were seeded in 6-well plates at a density of 500 cells per well. Following an overnight incubation of seeded plates, the indicated cells were

treated with various concentration of **16h** for 72 h and the cells were further cultured with complete medium for 10 days. The treated cells were analyzed by colony formation assay, as described previously [42].

4.2.5. Western blot assay

The expression level of cellular proteins of interest was determined using Western blotting analysis. Immunoblotting analysis was performed according to previously published procedures [42-44]. Blots were imaged by ChemiDoc™ MP Imaging System (Bio-Rad Laboratories, Inc., California, USA).

4.2.6. Cell cycle analysis

Cell-cycle analysis was conducted by propidium iodide (PI) staining. Cell cycle analysis was analyzed after **16h** treatment for 24 h. Briefly, cells were plated in culture dishes and cultured with fresh medium without FBS for 12 h. Then, cells were treated with **16h** for 24 h and remove the supernatant, the treated cells were fixed with 70% ethanol overnight before staining with propidium iodide mixed with RNase. Keep the dying cells under dark conditions at room temperature for 30 min before being subjected to flow cytometry analysis.

4.2.7. Apoptosis analysis

Apoptosis was detected by flow cytometry using Annexin V-FITC according to the manufacturer's protocol (BD Biosciences). MDA-MB-231 cells were treated with **16h** for 48 h before Annexin V and propidium iodide (PI) staining. Keep the dying cells under dark conditions at room temperature for 15 min before being subjected to flow cytometry analysis.

4.2.8. Molecular modeling

Molecular docking was performed according to the previous study [40]. The crystal structure of Aurora A (PDB entry code: 3P9J) in complex with EGJ was used for molecular modeling. The AutoDock 4.2 was employed for docking calculations. The protein optimization of Aurora A kinase was carried out using Sybyl 7.3. Docking parameters and fragmental volumes for the proteins were assigned using the addsol utility in the AutoDock 4.2 program. The size of energy grid box was set to A 60 × 60 × 60 Å with a grid spacing of 0.375 Å based on its cocrystallization ligand. Affinity grid fields were generated using the auxiliary program AutoGrid 4.0. The Lamarckian genetic algorithm (LGA) was used to find the appropriate binding positions, orientations, and conformations of the ligands. In each group, the lowest binding energy configuration with the highest% frequency was selected as the group representative. Accelrys Discovery Studio Visualizer 4.5 was used for graphic display.

4.2.9. Statistical Analysis

The data are presented as the mean ± SD for the indicated number of independently performed experiments. Statistical significance (*p <0.05, **p < 0.01, or ns [not significant]) was assessed using Student's t test.

Conflict of interest

The authors declare no competing financial interest.

Acknowledgements

This work was supported by the Natural Science Foundation of China (Grants 21907020) and the Natural Science Foundation of Guizhou Province (QKH

[2019]1215). This manuscript was edited for proper English language, grammar, punctuation, spelling, and overall style by one or more of the highly qualified native English-speaking editors at American Journal of Experts.

References

[1] S. Fu, Y. Li, J. Huang, T. Liu, Aurora kinase inhibitor VE 465 synergistically enhances cytotoxicity of carboplatin in ovarian cancer cells through induction of apoptosis and downregulation of histone 3, Cancer Bio. Ther. 13 (2012) 1034-1041.

[2] C. Lindon, R. Grant, M. Min, Ubiquitin-Mediated Degradation of Aurora Kinases, Front Oncol. 5 (2016) 307.

[3] A. Hutterer, D. Berdnik, F. Wirtz-Peitz, M. Zigman, Mitotic activation of the kinase Aurora-A requires its binding partner Bora, Dev. Cell, 11 (2006) 147-157.

[4] O. Gautschi, J. Heighway, P.C. Mack, P.R. Purnell, Aurora Kinases as Anticancer Drug Targets, Clin. Cancer Res. 14 (2008) 1639-1648.

[5] M. Yan, C. Wang, B. He, M. Yang, Aurora□A Kinase: A Potent Oncogene and Target for Cancer Therapy, Med. Res. Rev. 36 (2016) 1036-1079.

[6] A.P. Damodaran, L. Vaufrey, O. Gavard, C. Prigent, Aurora A Kinase Is a Priority Pharmaceutical Target for the Treatment of Cancers, Trends Pharmacol. Sci. (2017) S0165614717301116.

[7] Y. Xie, S. Zhu, M. Zhong, M. Yang, Inhibition of Aurora Kinase A Induces Necroptosis in Pancreatic Carcinoma, Gastroenterology, 153 (2017) S001650851735967X.

[8] S.S. Chang, H. Yamaguchi, W. Xia, S.O. Lim, Aurora A kinase activates YAP signaling in triple-negative breast cancer, Oncogene 36 (2016) 1265.

[9] Y. Nadler, R.L. Camp, C. Schwartz, D.L. Rimm, Expression of Aurora A (but not Aurora B) is predictive of survival in breast cancer, Clin. Cancer Res. 14 (2008) 4455-4462.

[10] R. Toughiri, Discovery of Aurora-A kinase physiological substrates in prostate cancer cells, Dissertations & Theses-Gradworks (2013).

[11] R. Toughiri, X. Li, Q. Du, C.J. Bieberich, Phosphorylation of NuMA by Aurora-A kinase in PC-3 prostate cancer cells affects proliferation, survival, and interphase NuMA localization, J. Cell. Biochem. 114 (2013) 823-830.

[12] M. Castedo, J.L. Perfettini, T. Roumier, K. Andreau, Cell death by mitotic catastrophe: a molecular definition, Oncogene 23 (2004) 2825-2837.

[13] J.W. Cheong, H.I. Jung, J.I. Eom, S.J. Kim, Aurora-A kinase inhibition enhances the cytosine arabinoside-induced cell death in leukemia cells through apoptosis and mitotic catastrophe, Cancer Lett. 297 (2010) 171-181.

[14] R.M. Scaife, G2 cell cycle arrest, down-regulation of cyclin B, and induction of mitotic catastrophe by the flavoprotein inhibitor diphenyleneiodonium, Mol. Cancer Ther. 3 (2004) 1229.

[15] A.C. Borisa, H.G. Bhatt, A comprehensive review on Aurora kinase: Small molecule inhibitors and clinical trial studies, Eur. J. Med. Chem. 140 (2017) 1-19.

[16] J. Yu, J. Zhou, F. Xu, W. Bai, High expression of Aurora-B is correlated with poor prognosis and drug resistance in non-small cell lung cancer, The International Journal of Biological Markers (2018) 172460081775309.

[17] M. Kamran, Z.J. Long, D. Xu, S.S. Lv, Aurora kinase A regulates Survivin stability through targeting FBXL7 in gastric cancer drug resistance and prognosis, Oncogenesis, 6 (2017)

298-310.

[18] Z. Zou, Z. Yuan, Q. Zhang, Z. Long, Aurora kinase A inhibition-induced autophagy triggers drug resistance in breast cancer cells, Autophagy, 8 (2012) 1798-1810.

[19] K.N. Shah, R. Bhatt, J. Rotow, J. Rohrberg, Aurora kinase A drives the evolution of resistance to third-generation EGFR inhibitors in lung cancer, Nat. Med. 25 (2019) 111-118.

[20] H. Liu, D. Zhang, A. Borczuk, V. Chau, Abstract 1217: Blockade of Aurora kinase A synergizes with platinum and radiation in non-small cell lung cancer cells, Cancer Res. 77 (2017) 1217-1217.

[21] Y. Li, W. Zhou, K. Tang, X. Chen, Silencing Aurora A leads to re-sensitization of breast cancer cells to Taxol through downregulation of SRC-mediated ERK and mTOR pathways, Oncol. Rep. 38 (2017) 2011-2022.

[22] M.S. Phadke, P. Sini, K.S.M. Smalley, The novel ATP-competitive MEK/Aurora kinase inhibitor BI-847325 overcomes acquired BRAF inhibitor resistance through suppression of Mcl-1 and MEK expression, Mol. Cancer Ther. 14 (2015) 1354-1364.

[23] M.E. Prime, S.M. Courtney, F.A. Brookfield, R.W. Marston, V. Walker, Phthalazinone pyrazoles as potent, selective, and orally bioavailable inhibitors of aurora-a kinase, J. Med. Chem. 54 (2011) 312-319.

[24] X.j. Wang, A.L. Sinn, P. Karen, S. George, Preclinical activity of a novel multiple tyrosine kinase and aurora kinase inhibitor, ENMD-2076, against multiple myeloma, Br. J. Haematol, 150 (2010) 313-325.

[25] M.G. Manfredi, J.A. Ecsedy, K.A. Meetze, S.K. Balani, O. Burenkova, Antitumor activity of MLN8054, an orally active small-molecule inhibitor of Aurora A kinase, Proc. Natl. Acad.

Sci .USA, 104 (2007) 4106-4111.

[26] F. Daniele, M. Jürgen, V. Mario, B. Rodrigo, 1,4,5,6-Tetrahydropyrrolo[3,4-c]pyrazoles: Identification of a Potent Aurora Kinase Inhibitor with a Favorable Antitumor Kinase Inhibition Profile, J. Med. Chem. 49 (2006) 7247-7251.

[27] S. Wang, C. A. Midgley, F. Scaërou, J. B. Grabarek, Discovery of N-Phenyl-4-(thiazol-5-yl)pyrimidin-2-amine Aurora Kinase Inhibitors, J. Med. Chem. 53 (2010) 4367-4378.

[28] S. Howard, V. Berdini, J. A. Boulstridge, M. G. Carr, Fragment-based discovery of the pyrazol-4-yl urea (AT9283), a multitargeted kinase inhibitor with potent aurora kinase activity, J. Med. Chem. 52 (2009) 379-388.

[29] V. Bavetsias, S. Crumpler, C. Sun, S. Avery, B. Atrash, A. Faisal, A.S. Moore, M. Kosmopoulou, N. Brown, P.W. Sheldrake, Optimization of Imidazo[4,5-B]Pyridine-Based Kinase Inhibitors: Identification of a Dual Flt3/Aurora Kinase Inhibitor as an Orally Bioavailable Preclinical Development Candidate for the Treatment of Acute Myeloid Leukemia, J. Med. Chem. 55 (2012) 8721.

[30] S. Hirai, H. Kikuchi, H. Kim, K. Begum, Metabolites of Febrifugine and It's Synthetic Analogue by Mouse Liver S9 and Their Antimalarial Activity against Plasmodium Malaria Parasite, J. Med. Chem. 46 (2003) 4351-4359.

[31] P.C. Sharma, G. Kaur, R. Pahwa, A. Sharma, Quinazolinone analogs as potential therapeutic agents, Curr. Med. Chem. 18 (2011) 4786-4812.

[32] Z. Malinowski, E. Fornal, M. Nowak, R. Kontek, Synthesis and biological evaluation of some amino- and sulfanyl-3*H*-quinazolin-4-one derivatives as potential anticancer agents,

Monatshefte für Chemie-Chemical Monthly, 146 (2015) 1723-1731.

[33] V. Bavetsias, L.A. Skelton, F. Yafai, F. Mitchell, The Design and Synthesis of Water-Soluble Analogues of CB30865, a Quinazolin-4-one-Based Antitumor Agent, J. Med. Chem. 45 (2002) 3692-3702.

[34] C. Jean-Christophe, C. Francois, M. Hervé, S. Laurent, M. Jacques, N. Anil, P. Eric, L. M. Ronan, D. Cécile and N. Jean-Paul, SAR156497, an Exquisitely Selective Inhibitor of Aurora Kinases, J. Med. Chem. 58 (2015) 1362-1375.

[35] R.R. Yadav, S.K. Guru, P. Joshi, G. Mahajan, 6-Aryl substituted 4-(4-cyanomethyl) phenylamino quinazolines as a new class of isoform-selective PI3K-alpha inhibitors, Eur. J. Med. Chem. 122 (2016) 731-743.

[36] H. Zhang, M. Xin, X. Xie, S. Mao, Synthesis and antitumor activity evaluation of PI3K inhibitors containing 3-substituted quinazolin-4(3*H*)-one moiety, Bioorgan. Med. Chem. 23 (2015) 7765–7776.

[37] F. Li, B. Frett, H.Y. Li, Selective Reduction of Halogenated Nitroarenes with Hydrazine Hydrate in the Presence of Pd/C, Synlett. 25 (2014) 1403-1408.

[38] R. Frei, A.S. Breitbach, H.E. Blackwell, 2-Aminobenzimidazole Derivatives Strongly Inhibit and Disperse Pseudomonas aeruginosa Biofilms, Angew. Chem. Int. Edit. 51 (2012) 5226-5229.

[39] A. Kamal, D. Busch, T. Phuong, J. Sensintaffar, Aurora kinase inhibition-dissecting cellular mechanisms, Cancer Lett. 66 (2006) 490-490.

[40] Y.H. Fan, H.Y. Lu, H.D. Ma, F. Feng, Bioactive compounds of Eriocaulon sieboldianum blocking proliferation and inducing apoptosis of HepG2 cells might be involved in Aurora

kinase inhibition, Food Funct. 6 (2015) 3746-3759.

[41] J.P. Li, Y.X. Yang, Q.L. Liu, S.T. Pan, The investigational Aurora kinase A inhibitor alisertib (MLN8237) induces cell cycle G2/M arrest, apoptosis, and autophagy via p38 MAPK and Akt/mTOR signaling pathways in human breast cancer cells, Drug Des. Devel. Ther. 9 (2015) 1627-1652.

[42] Y.H. Fan, H.W. Ding, D. Kim, D. Bach, Antitumor Activity of DFX117 by Dual Inhibition of c-Met and PI3Kα in Non-Small Cell Lung Cancer, Cancers, 11 (2019) 627-647.

[43] Y.H. Fan, H.W. Ding, D.D. Liu, H.R. Song, Novel 4-aminoquinazoline derivatives induce growth inhibition, cell cycle arrest and apoptosis via PI3Kα inhibition, Bioorgan. Med. Chem. 26 (2018) 1675-1685.

[44] Y.H. Fan, W. Li, D.D. Liu, M.X. Bai, Design, synthesis, and biological evaluation of novel 3-substituted imidazo[1,2-*a*]pyridine and quinazolin-4(3*H*)-one derivatives as PI3Kα inhibitors, Eur. J. Med. Chem. 136 (2017) 95-106.

Highlights:

- A novel series of 6-(2-amino-1*H*-benzo[*d*]imidazol-6-yl)quinazolin-4(3*H*)-one derivatives were designed and synthesised.
- **16h** showed the most potent Aurora A kinase inhibitory activity with IC_{50} values of 21.94 nM.
- **16h** caused aberrant mitotic phenotypes and obvious G2/M phase arrest in MDA-MB-231 cells.
- **16h** induced cell apoptosis via a caspase-dependent pathway in MDA-MB-231 cells.

Declaration of interests

☒ The authors declare that they have no known competing financial interests or personal relationships that could have appeared to influence the work reported in this paper.

☐The authors declare the following financial interests/personal relationships which may be considered as potential competing interests: